NASA Technical Memorandum 4363

Measurements of Fluctuating Pressure in a Rectangular Cavity in Transonic Flow at High Reynolds Numbers

M. B. Tracy, E. B. Plentovich,
and Julio Chu
Langley Research Center
Hampton, Virginia

National Aeronautics and
Space Administration
Office of Management
Scientific and Technical
Information Program
1992

Abstract

An experiment was performed in the Langley 0.3-Meter Transonic Cryogenic Tunnel to study the internal acoustic field generated by rectangular cavities in transonic and subsonic flows and to determine the effect of Reynolds number and angle of yaw on the field. The cavity in this study was 11.25 in. long and 2.50 in. wide. The cavity depth was varied to obtain length-to-height (l/h) ratios of 4.40, 6.70, 12.67, and 20.00. Data were obtained for a free-stream Mach number (M_∞) range from 0.20 to 0.90, a Reynolds number range from 2×10^6 to 100×10^6 per foot with a nearly constant boundary-layer thickness, and for two angles of yaw of 0° and 15°. Results show that Reynolds number has little effect on the acoustic field in rectangular cavities at an angle of yaw of 0°. Cavities with $l/h = 4.40$ and 6.70 generated tones at transonic speeds, whereas those with $l/h = 20.00$ did not. This trend agrees with data obtained previously at supersonic speeds. As M_∞ decreased, the amplitude and bandwidth of the tones changed. No tones appeared for $M_\infty = 0.20$. For a cavity with $l/h = 12.67$, tones appeared at $M_\infty = 0.60$, indicating a possible change in flow-field type. Changes in acoustic spectra with angle of yaw varied with Reynolds number, M_∞, l/h ratios, and acoustic mode number.

Introduction

Carrying weapons internally provides aerodynamic advantages in flight; however, difficulties such as large nose-up pitching moments or store structural vibration can arise when a store is required to separate from a cavity exposed to an external flow. To ensure safe separation of a store exiting from a cavity, it is necessary to study the flow disturbances generated when a rectangular cavity is introduced into uniform flow. In addition to changes in the mean pressure distribution in the cavity, an acoustic pressure field with high-intensity tones that radiate from the cavity can occur as reported in references 1–10. This paper addresses acoustic tone generation under transonic and subsonic conditions.

Four types of flow have been observed for cavities under supersonic conditions: closed, open, transitional-closed, and transitional-open. (See, for example, refs. 11 and 12.) Closed cavity flow, in which the shear layer attaches to the floor of the cavity, is observed for cavities with length-to-height (l/h) ratios greater than 13 at supersonic speeds. Such flow produces an adverse static pressure gradient in the cavity that causes a separating store to experience large nose-up pitching moments. Open cavity flow, in which the shear layer bridges the cavity, is seen at supersonic speeds for cavities with l/h ratios less than 10. Although this type of flow produces a more uniform static pressure distribution, it is this flow regime that can produce high-intensity acoustic tones. Transitional-closed and transitional-open flows are two distinct transitional flows for which the corresponding acoustic fields have not been determined.

The mechanism that produces the acoustic tones is understood to be a reinforcement between instabilities in the shear layer that bridges the cavity and pressure waves generated in the cavity when the shear layer impinges on the aft wall. Acoustic tones occur at discrete frequencies that correspond to characteristic pressure patterns (standing waves or modes) in the cavity. Although there is no satisfactory method to predict tone amplitude (or whether they will occur), the frequencies at which the tones may occur can be predicted by a semiempirical equation determined by Rossiter in reference 1 and modified by Heller, Holmes, and Covert in reference 2. The modified Rossiter equation, which is described later, depends on cavity dimensions and flow speed.

The purpose of this study was to determine if tones are generated at transonic speeds for the same geometries (l/h ratios) as at supersonic speeds and to determine the effect of Reynolds number (apart from boundary-layer thickness) and angle of cavity yaw on the internal acoustic fields.

Symbols and Abbreviations

FPL	fluctuating pressure level, dB re q_∞
f	frequency, Hz
f_m	frequency of acoustic mode, Hz
h	cavity height, in.

$k(M_\infty)$	empirical ratio of shear layer and free-stream velocities
l	cavity length (11.25 in.), in.
M_∞	free-stream Mach number
m	acoustic mode number
p	measured fluctuating pressure, psf
$p_{t,\infty}$	free-stream total pressure, psi
q_∞	free-stream dynamic pressure, psf
R_∞	free-stream unit Reynolds number per foot
$T_{t,\infty}$	free-stream total temperature, K
U_∞	free-stream velocity, fps
x	longitudinal distance from origin, in.
y	lateral distance from origin, in.
z	vertical distance from origin, in.
$\alpha(l/h)$	empirical phase between instabilities in shear layer and pressure waves
γ	ratio of specific heat of test gas at constant pressure to that at constant volume
ψ	angle of yaw, deg

Experimental Description

Test Facility

The experimental study was performed in the 13- by 13-in. test section of the Langley 0.3-Meter Transonic Cryogenic Tunnel (0.3-m TCT) shown in figure 1. (Refs. 13 and 14 describe the facility and operation in more detail.) The 0.3-m TCT is a continuous-flow, fan-driven, cryogenic pressure tunnel that uses nitrogen as a test gas. All the walls of the test section are solid. The sidewalls are rigid, whereas the top and bottom walls are flexible and movable. The latter are computer controlled, given feedback on wall position and pressure distribution, to achieve alignment with model streamlines. This is done so that the flow in the vicinity of the model will be the same as that obtained for the free-stream condition. Reference 15 gives a more detailed description of the adaptive walls.

The Mach number in the tunnel can be varied continuously from 0.20 through 0.95. The stagnation pressure and temperature are variable from 1.2 to 6.0 atm and 80 K to 320 K, respectively, which permits unit Reynolds numbers up to 100×10^6 per foot.

Model

A rectangular cavity model was mounted on a turntable that was installed in the sidewall of the 0.3-m TCT. Figure 2 shows the cavity with dynamic pressure instrumentation prior to installation in the tunnel. The cavity was 11.25 in. long by 2.50 in. wide and the depth was variable to obtain l/h ratios of 4.40 ($h = 2.56$ in.), 6.70 ($h = 1.68$ in.), 12.67 ($h = 0.89$ in.), and 20.00 ($h = 0.56$ in.). The turntable could be rotated with respect to the flow to position the cavity with angles of yaw of 0° and 15°.

Instrumentation

The model was instrumented with 18 dynamic pressure transducers (16 of which were along the centerline and 1 each on the fore and aft walls at half-depth) as shown schematically in figure 3. The origin of the coordinates used was the center top of the forward cavity wall. The transducers were miniature, high-sensitivity, piezoresistive, differential dynamic pressure transducers with a full-scale range of ±10 psid and a resonant frequency of 130 000 Hz. Transducer 8 was sealed to determine the sensitivity of the transducer to vibration, which proved to be negligible. The reference pressure was local static pressure. (Transducers 1–3 and 15–17 were manifolded to a static pressure port identified as SR1 in figure 3; transducers 4–11 were manifolded to SR2; and transducers 12–14, 18, and 19 were manifolded to SR3.) A 1000-Hz bench calibration verified that the temperature compensation maintained a sensitivity that was within ±10 percent of a reference sensitivity at 100 K. Analog data were recorded on two 14-channel FM tape recorders using a medium band format at 30 in/sec (0–10 kHz). A sine wave calibration was applied to each pressure transducer several times throughout the test.

Test Matrix

Data were obtained for $M_\infty = 0.20$, 0.60, 0.80, and 0.90. The Reynolds number was varied from 4×10^6 to 100×10^6 per foot at angles of yaw of 0° and 15°.

Boundary-Layer Thickness

Because boundary-layer thickness is an important parameter in cavity flows (refs. 16 and 17) and because it varies with Reynolds number, the effect of Reynolds number was isolated from that of boundary-layer thickness. For this experiment, a

nearly constant boundary-layer thickness was maintained for the range of test Reynolds numbers. The thickness of the boundary layer at the leading edge of the cavity was determined with measurements made with a total pressure rake by using a method described in reference 18. The boundary-layer thickness is defined as the distance from the surface at which the boundary-layer velocity equals 99 percent of the free-stream velocity. For $M_\infty = 0.60$, the boundary-layer thickness was found to range from 0.58 in. at $R_\infty = 5 \times 10^6$ per foot to 0.47 in. at $R_\infty = 85 \times 10^6$ per foot; and for $M_\infty = 0.90$, it ranged from 0.51 in. at $R_\infty = 13 \times 10^6$ per foot to 0.49 in. at $R_\infty = 100 \times 10^6$ per foot. Measurements were made with the cavity floor positioned flush with the turntable ($h = 0.00$ in.).

Data Analysis

An antialiasing filter was applied at 5 kHz and the analog data were sampled at 12.5 kHz. The digitized data were divided into 50 blocks (assumed independent) of 4096 points each. Each block was Fourier analyzed by using a Hanning window and the resulting spectra were averaged. This process produced spectra with a frequency resolution of 3 Hz and 95-percent confidence that the spectral estimate was within ±1 dB of the true spectra based on a chi-square distribution.

Results and Discussion

Since the data were obtained for a wide range of temperatures and dynamic pressures, the data were nondimensionalized by using free-stream parameters. The fluctuating pressure is presented in decibels (dB) as is customary for acoustic data and is nondimensionalized with free-stream dynamic pressure as is customary for aerodynamic data. The fluctuating pressure level is defined as follows:

$$\mathrm{FPL} = 20 \log \frac{p}{q_\infty}$$

Frequency is nondimensionalized by using the cavity length l and the free-stream flow speed U_∞.

The acoustic tones that radiated from the cavity corresponded to characteristic pressure patterns (standing waves or acoustic modes) in the cavity. An illustration of an acoustic mode shape in the cavity can be obtained by plotting the amplitude of a tone, at a given frequency, as a function of position along the length of the cavity. Figure 4 presents three different mode shapes (corresponding to $fl/U_\infty \approx 0.7$, 1.1, and 1.5) in a cavity with $l/h = 6.70$, $M_\infty = 0.80$, $\psi = 0°$, and $R_\infty = 99 \times 10^6$ per foot. The acoustic mode shapes were similar to those observed in organ pipes but were somewhat elongated, as if the downstream wall was soft. Subsequent data are presented as acoustic spectra. Data from transducer 1 (see fig. 3) are used in this report as they are representative of data obtained throughout the cavity but contained the least amount of broadband noise (tones appeared higher against the background in the spectra). Except where indicated, all data are presented for an angle of yaw of 0°. For reference, a set of nondimensional modal frequencies predicted by the modified Rossiter equation (see refs. 1 and 2), which is given here as

$$f_m \frac{l}{U_\infty} = \frac{m - \alpha\,(l/h)}{M_\infty \left[1 - \left(\frac{\gamma-1}{2}\right) M_\infty^2\right]^{-1/2} + k\,(M_\infty)}$$

are given in chart A where, from reference 1,

$$\gamma = 1.4$$

$$\alpha(l/h) = 0.25 \qquad (l/h = 4.00)$$

$$k(M_\infty) = 0.57 \qquad (M_\infty = 0.40\text{–}1.20)$$

Chart A

Mode	Nondimensional modal frequencies at a Mach number of —			
	0.20	0.60	0.80	0.90
1	0.38	0.32	0.30	0.29
2	.90	.75	.70	.68
3	1.41	1.18	1.10	1.06
4	1.92	1.61	1.50	1.45
5	2.44	2.04	1.90	1.84
6	2.95	2.47	2.30	2.22
7	3.46	2.90	2.70	2.61

The coefficients α and k used in the equation were published values (ref. 1) obtained for $l/h = 4.00$ and $M_\infty = 0.40$ through 1.20, respectively. A summary of the test points for which tones were observed is included in the nominal test matrix given in table 1.

Effect of l/h

One of the main objectives of this study was to determine if the tones that correspond to the predicted Rossiter frequencies are generated by cavities with the same l/h ratios at transonic speeds as they are at supersonic speeds. Figure 5 presents plots comparing FPL spectra for the four l/h configurations at $M_\infty = 0.60, 0.80$, and 0.90 and for the highest Reynolds number obtained (85×10^6, 100×10^6, and 100×10^6 per foot, respectively). The modal frequencies predicted by the modified Rossiter equation (for $l/h = 4.00$ and $M_\infty = 0.40$–1.20) are indicated by bold tick marks on the abscissa. As discussed in reference 19, the modified Rossiter equation is a semiempirical equation that was determined for a limited parameter range. These limitations may account for the disagreement between the predicted modal frequencies and those observed in this test.

Figure 5 illustrates that the deeper the cavity (or greater the volume), the greater the acoustic pressures. Tones were observed for cavities with $l/h = 4.40$ and 6.70 but not 20.00, which agrees with data obtained previously under supersonic conditions (ref. 20). The tones that appear in figure 5 for $l/h = 20.00$ coincide with the tunnel fan blade passing frequency and first harmonic; $fl/U_\infty = 1.21$ and 2.42, for $M_\infty = 0.60$; $fl/U_\infty = 1.13$ and 2.26 for $M_\infty = 0.80$; and $fl/U_\infty = 1.07$ and 2.14 for $M_\infty = 0.90$. An unanticipated result was the presence of tones for $l/h = 12.67$ at $M_\infty = 0.60$ but not at $M_\infty = 0.80$ or 0.90, which indicated a possible change in flow field.

Data for $M_\infty = 0.20$ were available only for $l/h = 4.40$ and 6.70. There were no tones apparent and no notable differences between the spectra.

Effect of Reynolds Number

As indicated before, a nearly constant boundary-layer thickness was maintained for the test range of Reynolds numbers. Figures 6, 7, and 8 illustrate the effect of Reynolds number on the cavity FPL for each l/h configuration at $M_\infty = 0.60, 0.80$, and 0.90, respectively. Little change occurred with changing Reynolds number. The tones, the significant features in the spectra, did not change in amplitude, bandwidth, or center frequency (modal frequency) as the Reynolds number changed. Data for $M_\infty = 0.20$ were available only for low Reynolds numbers (less than 30×10^6 per foot) and are not presented.

Effect of Mach Number

Mode amplitude and bandwidth changed with Mach number. Different tones dominated the spectra for different Mach numbers. Figure 9 gives the spectra and compares the cavity FPL with the Mach number range for each l/h configuration at $\psi = 0°$ and $R_\infty = 30 \times 10^6$ per foot.

For cavities with $l/h = 4.40$ and 6.70 (figs. 9(a) and (b), respectively), $M_\infty = 0.20$ spectra contained no identifiable features. The $M_\infty = 0.60$ spectra contained broad peaks. As the Mach number increased to 0.80, the second mode ($fl/U_\infty \approx 0.7$) sharpened and became dominant, whereas higher order modes ($fl/U_\infty \geq 1.2$) decreased in amplitude. Spectra for $M_\infty = 0.90$ were similar to the $M_\infty = 0.80$ spectra with the exception that the second mode which was prominent at $M_\infty = 0.80$ decreased in amplitude and the first mode ($fl/U_\infty \approx 0.3$) became more prominent. The broadening of the tones (i.e., high-pressure levels over a range of frequencies about the modal frequency) may indicate a destabilization of the feedback mechanism as the Mach number decreased.

Data from $l/h = 12.67$ (fig. 9(c)) showed the most dramatic change, indicating a possible change in flow-field type. The tones were eliminated as the Mach number increased from 0.60 to 0.80. Static pressure distributions (see ref. 19) are expected to aid in identifying the flow-field types at each Mach number.

Spectra for $l/h = 20.00$ (fig. 9(d)) contain no tones and show only a slight increase in broadband noise with increasing Mach number.

Effect of Yaw

Changes in the cavity fluctuating pressures with angle of yaw varied with Reynolds number, Mach number, l/h, and mode number. In no case were the tones eliminated altogether, which would have indicated a change from open to closed cavity type of flow. Except where noted later, the frequencies at which tones were observed coincided for both angles of yaw. Figures 10, 11, and 12 give spectra comparing data for angles of yaw of 0° and 15° for cavities with $l/h = 4.40, 6.70$, and 12.67, respectively. Each figure presents data for high and low Reynolds numbers at $M_\infty = 0.60, 0.80$, and 0.90.

The effect of yaw coupled with Reynolds number is most clearly seen when comparing figure 10(c) with 10(d), in which case there is a significantly

different decrease in amplitude of the second mode ($fl/U_\infty \approx 0.8$) with angle of yaw. Comparing figure 10(a) with 10(c) and figure 10(b) with 10(d) shows how Mach number can couple with yaw to either increase or decrease tone amplitude. There were cases in which tones appeared or disappeared with yaw. An example of the former case is the third mode ($fl/U_\infty \approx 1.1$) in figure 10(d). The latter case is seen for the first mode ($fl/U_\infty \approx 0.3$) in figure 11(f).

An interesting phenomenon is observed at $M_\infty = 0.90$, as seen in figures 10(e), 10(f), 11(e), and 11(f). Beginning with the third mode ($fl/U_\infty \approx 1.1$), there is a shift down (to the left) in the higher modal frequencies with increased yaw. This shift may result from the cavity appearing longer to the shorter wavelength modes when it is in the yawed position. (The apparent shift up in tone frequencies with yaw in fig. 10(c) was due to a slight difference in Mach number.)

As the cavity becomes more shallow, the effects described above become less dramatic for $l/h = 6.70$ and 12.67 cavities as seen in figures 11 and 12, respectively. No data are shown for the $l/h = 20.00$ configuration as there were no changes with yaw. The effect of yaw at $M_\infty = 0.20$ was minimal.

Concluding Remarks

An experiment was performed in the Langley 0.3-Meter Transonic Cryogenic Tunnel to study the internal acoustic field generated by rectangular cavities in transonic and subsonic flows and to determine the effect of Reynolds number and angle of yaw on the field. Reynolds number appeared to have little effect on the acoustic spectra generated by rectangular cavities at an angle of yaw of 0° for Mach numbers (M_∞) of 0.20 through 0.90.

Tones were observed for cavities with length-to-height (l/h) ratios of 4.40 and 6.70 but not 20.00, which agrees with data previously obtained under supersonic conditions. An unanticipated result was the presence of tones for $l/h = 12.67$ at $M_\infty = 0.60$. No tones appeared at $M_\infty = 0.80$ or 0.90 for $l/h = 12.67$.

Mode amplitude and bandwidth depended on Mach number. Prominent tones at $M_\infty = 0.80$ and 0.90 broadened and changed in amplitude as the Mach number decreased to 0.60. There were no tones apparent at $M_\infty = 0.20$ for any of the conditions or configurations tested.

The effect of yaw on cavity acoustics varied with Reynolds number, Mach number, l/h, and mode number. Higher order modes shifted down in frequency with yaw at $M_\infty = 0.90$.

NASA Langley Research Center
Hampton, VA 23665-5225
April 27, 1992

References

1. Rossiter, J. E.: *Wind-Tunnel Experiment on the Flow Over Rectangular Cavities at Subsonic and Transonic Speeds.* R. & M. No. 3438, British Aeronautical Research Council, Oct. 1964.

2. Heller, H. H.; Holmes, G.; and Covert, E. E.: *Flow-Induced Pressure Oscillations in Shallow Cavities.* AFFDL-TR-70-104, U.S. Air Force, Dec. 1970. (Available from DTIC as AD 880 496.)

3. Heller, Hanno H.; and Bliss, Donald B.: *Aerodynamically Induced Pressure Oscillations in Cavities—Physical Mechanisms and Suppression Concepts.* Tech. Rep. AFFDL-TR-74-133, U.S. Air Force, Feb. 1975.

4. Bartel, H. W.; and McAvoy, J. M.: *Cavity Oscillation in Cruise Missile Carrier Aircraft.* AFWAL-TR-81-3036, U.S. Air Force, June 1981. (Available from DTIC as AD A108 610.)

5. Clark, Rodney L.: *Evaluation of F-111 Weapon Bay Aeroacoustic and Weapon Separation Improvement Techniques.* AFFDL-TR-79-3003, U.S. Air Force, Feb. 1979. (Available from DTIC as AD A070 253.)

6. Kaufman, Louis G., II; Maciulaitis, Algirdas; and Clark, Rodney L.: *Mach 0.6 to 3.0 Flows Over Rectangular Cavities.* AFWAL-TR-82-3112, U.S. Air Force, May 1983. (Available from DTIC as AD A134 579.)

7. Shaw, Leonard; Clark, Rodney; and Talmadge, Dick: F-111 Generic Weapons Bay Acoustic Enviroment. AIAA-87-0168, Jan. 1987.

8. Gates, Roger S.; Butler, Carroll B.; Shaw, Leonard L.; and Dix, Richard E.: Aeroacoustic Effects of Body Blockage in Cavity Flow. AIAA-87-2667, Oct. 1987.

9. Shaw, Leonard; and Banaszak, Dave.: *Weapons Internal Carriage/Separation—"WICS" Aeroacoustic Research.* AFWAL-TM-86-243-FIBG, U.S. Air Force, Mar. 1987.

10. Dix, R. E.: *Weapons Internal Carriage and Separation at Transonic Conditions.* AEDC-TMR-89-P4, U.S. Air Force, Oct. 1989.

11. Wilcox, Floyd J., Jr.: Experimental Measurements of Internal Store Separation Characteristics at Supersonic Speeds. *Store Carriage, Integration and Release,* Royal Aeronautical Soc., 1990, pp. 5.1–5.16.

12. Stallings, Robert L., Jr.; and Wilcox, Floyd J., Jr.: *Experimental Cavity Pressure Distributions at Supersonic Speeds.* NASA TP-2683, 1987.

13. Ladson, Charles L.; and Ray, Edward J.: *Evolution, Calibration, and Operational Characteristics of the Two-Dimensional Test Section of the Langley 0.3-Meter Transonic Cryogenic Tunnel.* NASA TP-2749, 1987.

14. Rallo, Rosemary A.; Dress, David A.; and Siegle, Henry J. A.: *Operating Envelope Charts for the Langley 0.3-Meter Transonic Cryogenic Wind Tunnel.* NASA TM-89008, 1986.

15. Mineck, Raymond E.: *Hardware and Operating Features of the Adaptive Wall Test Section for the Langley 0.3-Meter Transonic Cryogenic Tunnel.* NASA TM-4114, 1989.

16. Rockwell, D.; and Naudascher, E.: Review—Self-Sustaining Oscillations of Flow Past Cavities. *Trans. ASME, Ser. I: J. Fluids Eng.*, vol. 100, no. 2, June 1978, pp. 152–165.

17. Komerath, N. M.; Ahuja, K. K.; and Chambers, F. W.: Prediction and Measurement of Flows Over Cavities—A Survey. AIAA-87-0166, Jan. 1987.

18. Plentovich, E. B.; Chu, Julio; and Tracy, M. B.: *Effects of Yaw Angle and Reynolds Number on Rectangular-Box Cavities at Subsonic and Transonic Speeds.* NASA TP-3099, 1991.

19. Dix, Richard E.; and Butler, Carroll: *Cavity Aeroacoustics.* AFATL-TP-90-08, U.S. Air Force, June 1990. (Available from DTIC as AD A223 853.)

20. Shaw, Leonard L.; and Reed, Gus: *Supersonic Flow Induced Cavity Acoustics.* AFWAL-TM-85-210, U.S. Air Force, Dec. 1985.

Table 1. Nominal Test Matrix and Presence of Tones

M_∞	R_∞ per foot	$p_{t,\infty}$, psi	$T_{t,\infty}$, K	$\psi = 0°$ with l/h of —					$\psi = 15°$ with l/h of —		
				4.40	6.70	12.67	20.00	∞ (a)	4.40	6.70	12.67
0.20	2×10^6	22.5	310	(b)	(b)				(b)	(b)	
	10	26	105	↓	↓				↓	↓	
	30	76	105								
0.60	4×10^6	19	320	(c)	(c)	(c)	(b)	(b)	(c)	(c)	(c)
	10	46	320								
	10	21	180						(c)	(c)	(c)
	30	64	180								
	30	30	105						(c)	(c)	(c)
	80	77	105						↓	↓	↓
	90	86	105	↓	↓	↓	↓	↓			
0.80	5×10^6	18	310	(c)	(c)	(b)	(b)	(b)	(c)	(c)	(b)
	10	37	310								
	10	21	200						↓	(c)	(b)
	30	62	200								
	30	26	105						(c)	(c)	(b)
	80	64	105								
	90	72	105								
	100	85	105	↓	↓	↓	↓	↓	↓	↓	↓
0.90	10×10^6	19.5	200	(c)	(c)	(b)	(b)	(b)	(c)	(c)	(b)
	30	68	200								
	30	22.5	105						(c)	(c)	(b)
	80	60	105								
	90	67	105						↓		
	100	75	105	↓	↓	↓	↓	↓		↓	↓

[a]Cavity ceiling flush with sidewall for boundary-layer measurements.
[b]No tones.
[c]Tones.

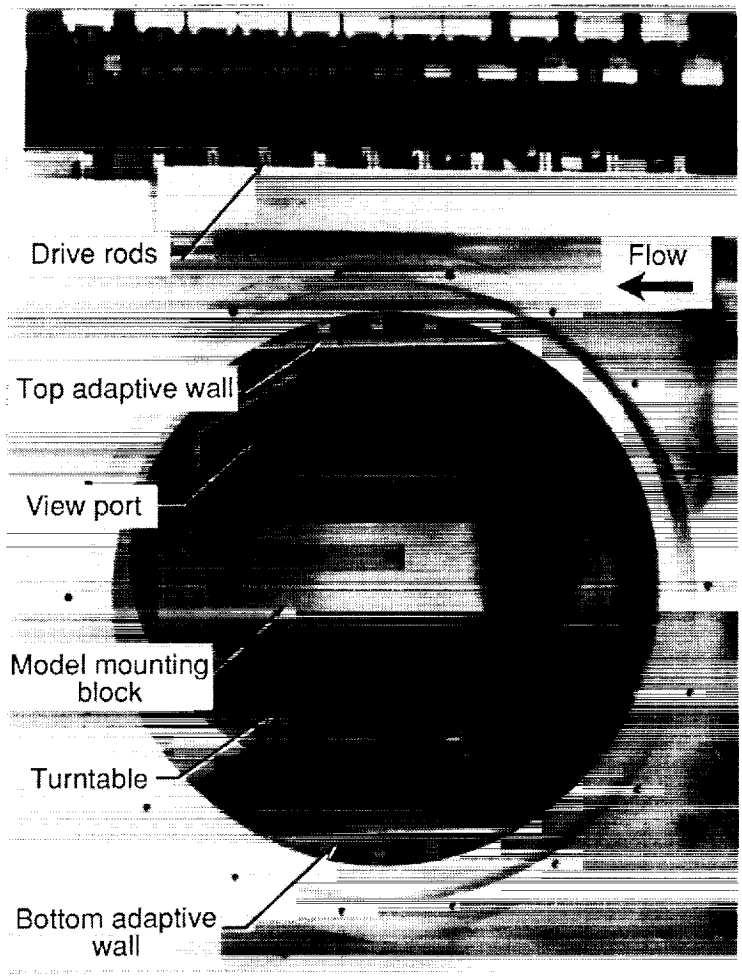

L-92-23

Figure 1. Interior of 13-in. by 13-in. test section of the Langley 0.3-m TCT.

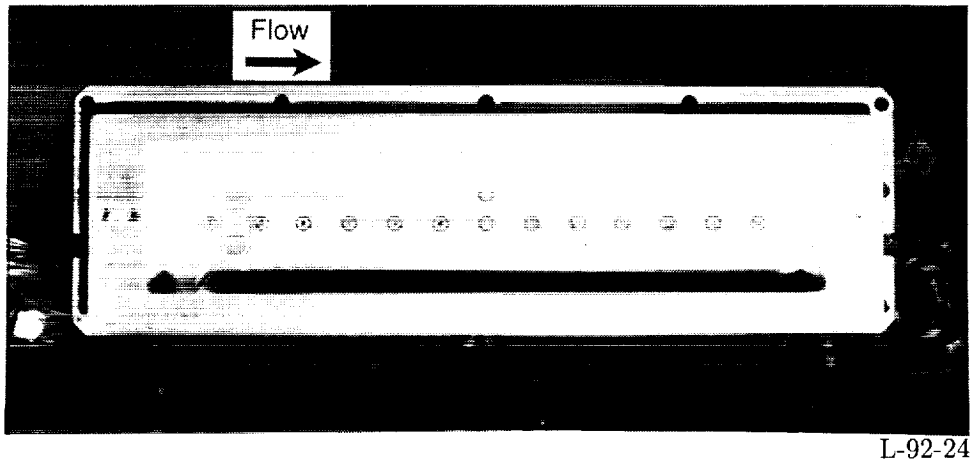

L-92-24

Figure 2. Rectangular cavity model for installation in sidewall of Langley 0.3-m TCT. Dynamic pressure transducers are shown.

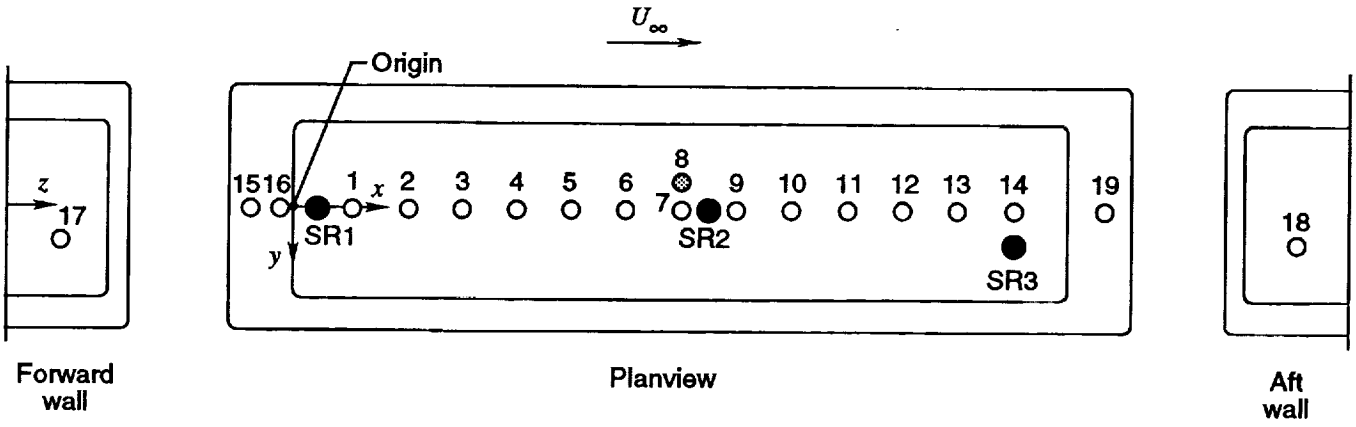

Transducer	x, in.	y, in.	z, in.	Model location	Reference port
1	0.800	0	h	Cavity floor	SR1
2	1.700				SR1
3	2.450				SR1
4	3.254				SR2
5	4.058				SR2
6	4.862				SR2
7	5.666	-.5			SR2
8	5.666	0			Sealed
9	6.470				SR2
10	7.274				SR2
11	8.078				SR2
12	8.882				SR3
13	9.686				SR3
14	10.490				SR3
15	-.690		0	Forward tunnel sidewall	SR1
16	-.230		0	Forward tunnel sidewall	SR1
17	0	.47	$h/2$	Forward cavity wall	SR1
18	11.250	.47	$h/2$	Aft cavity wall	SR3
19	11.800	0	0	Aft tunnel sidewall	SR3

Reference orifice	x, in.	y, in.	z, in.	Model location
SR1	0.401	0	h	Cavity floor
SR2	6.071	0	h	Cavity floor
SR3	10.486	.5	h	Cavity floor

Figure 3. Dynamic instrumentation layout. In the sketch, the open circles indicate open dynamic pressure transducers; the shaded circle indicates sealed pressure transducers; and the filled circles indicate static pressure orifices.

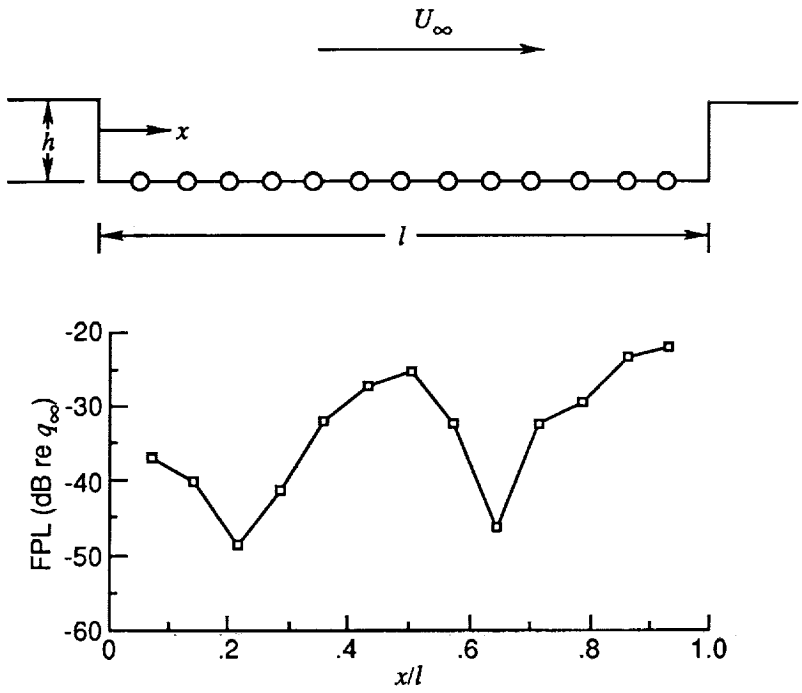

(a) Mode 2. $fl/U_\infty \approx 0.7$.

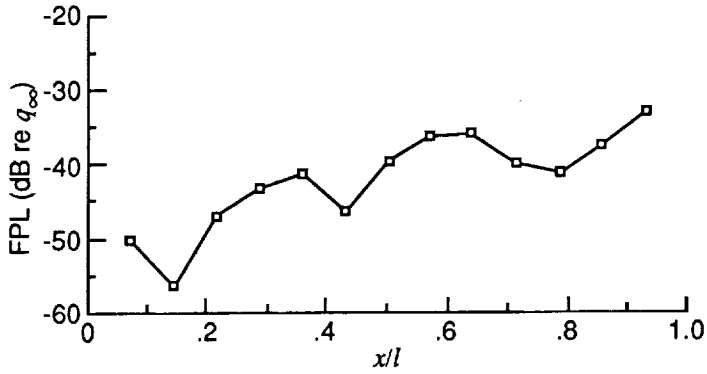

(b) Mode 3. $fl/U_\infty \approx 1.1$.

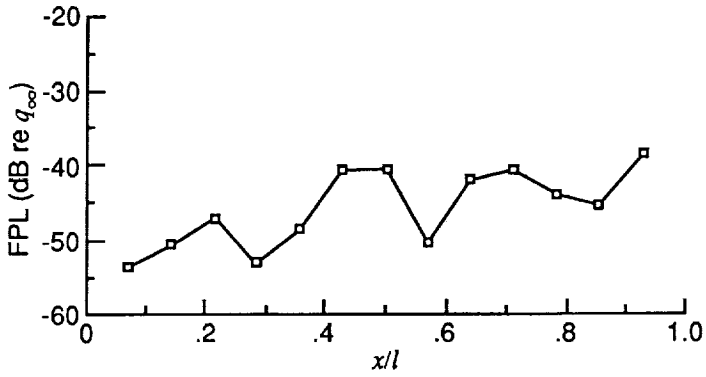

(c) Mode 4. $fl/U_\infty \approx 1.5$.

Figure 4. Mode shapes in cavity. $M_\infty = 0.80$; $\psi = 0°$; $l/h = 6.70$; $R_\infty = 99 \times 10^6$ per foot. Circles in top sketch indicate transducer locations.

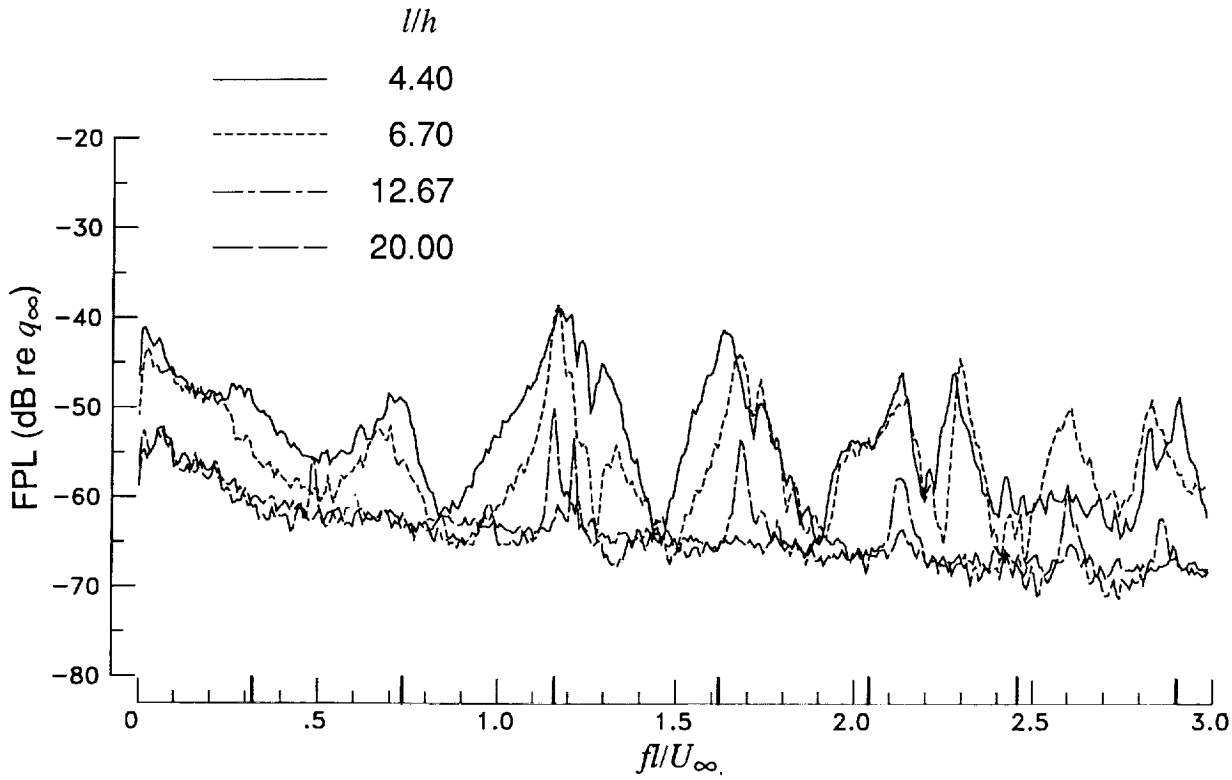

(a) $M_\infty = 0.60$; $R_\infty = 85 \times 10^6$ per foot. Fan blade passing frequency is 1.21.

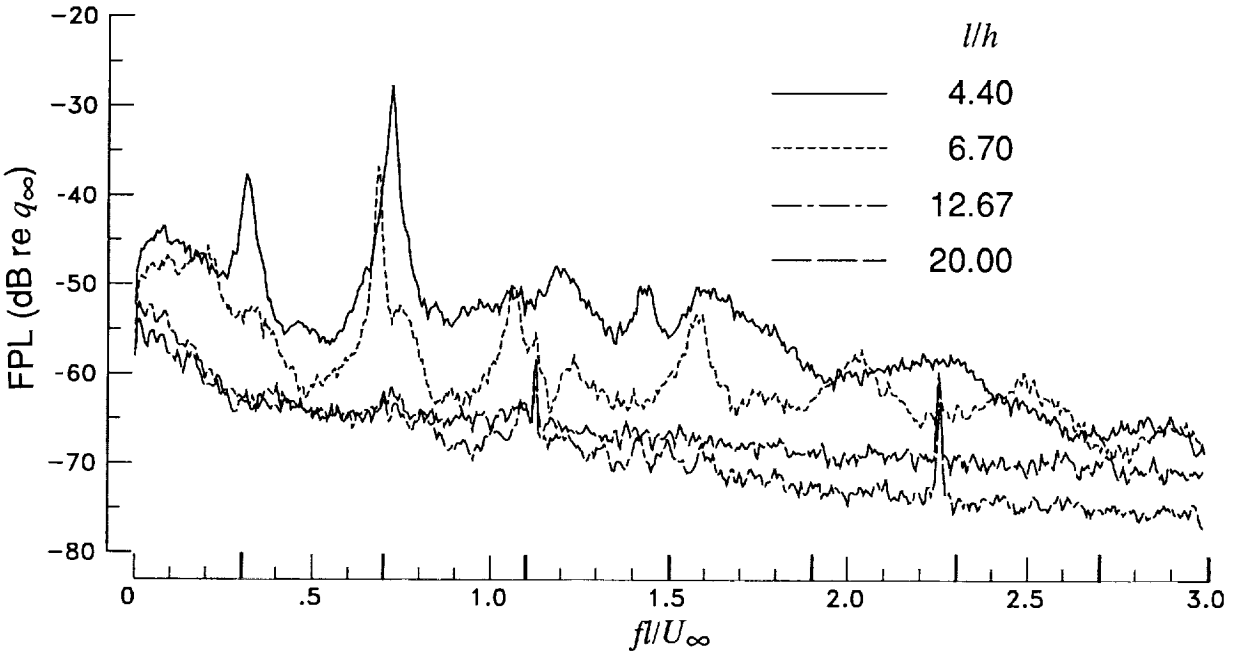

(b) $M_\infty = 0.80$; $R_\infty = 100 \times 10^6$ per foot. Fan blade passing frequency is 1.13.

Figure 5. Effect of l/h on cavity fluctuating pressures with $\psi = 0°$. Bold ticks on the abscissa indicate modal frequencies predicted by modified Rossiter equation.

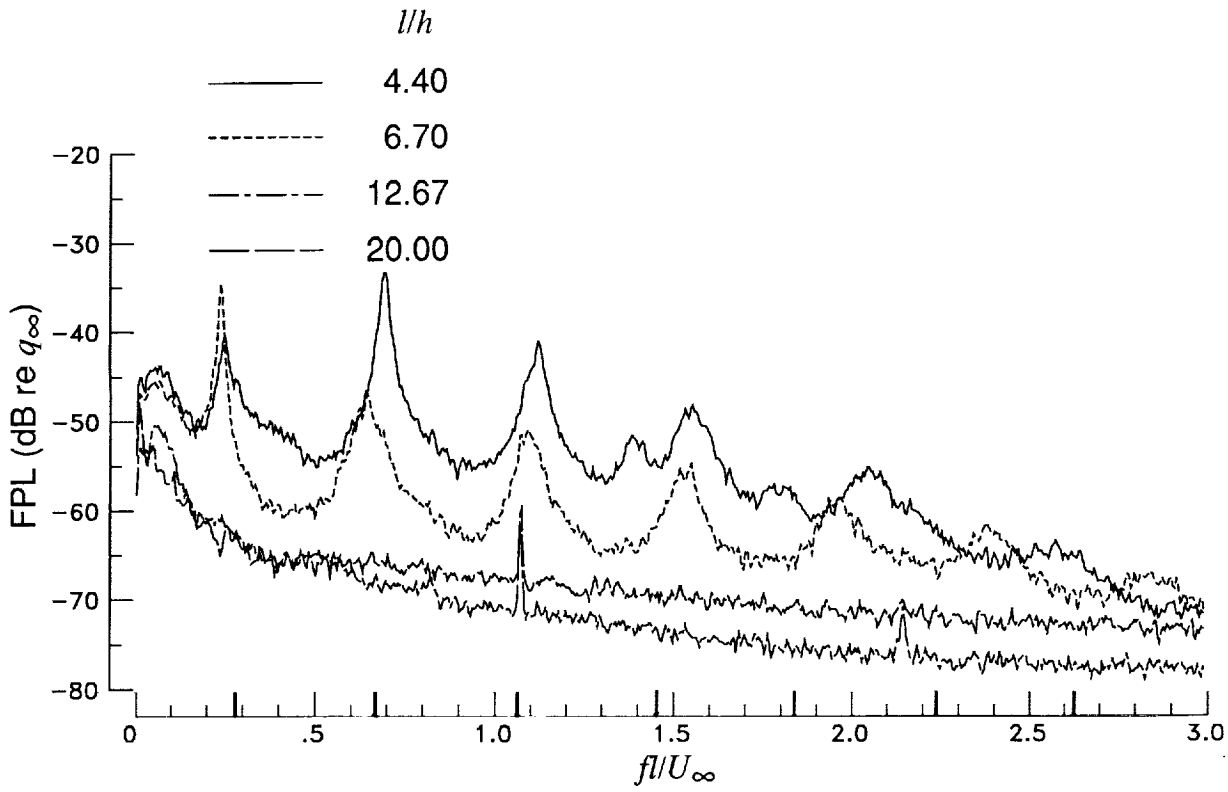

(c) $M_\infty = 0.90$; $R_\infty = 100 \times 10^6$ per foot. Fan blade passing frequency is 1.07.

Figure 5. Concluded.

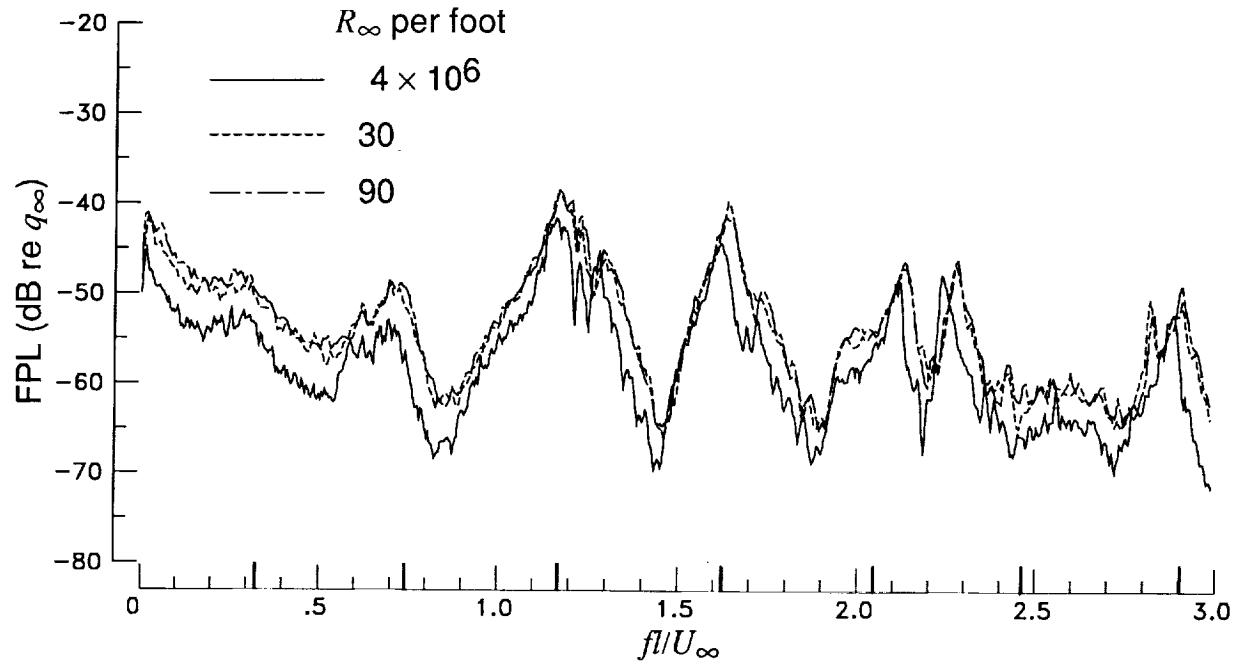

(a) $l/h = 4.40$.

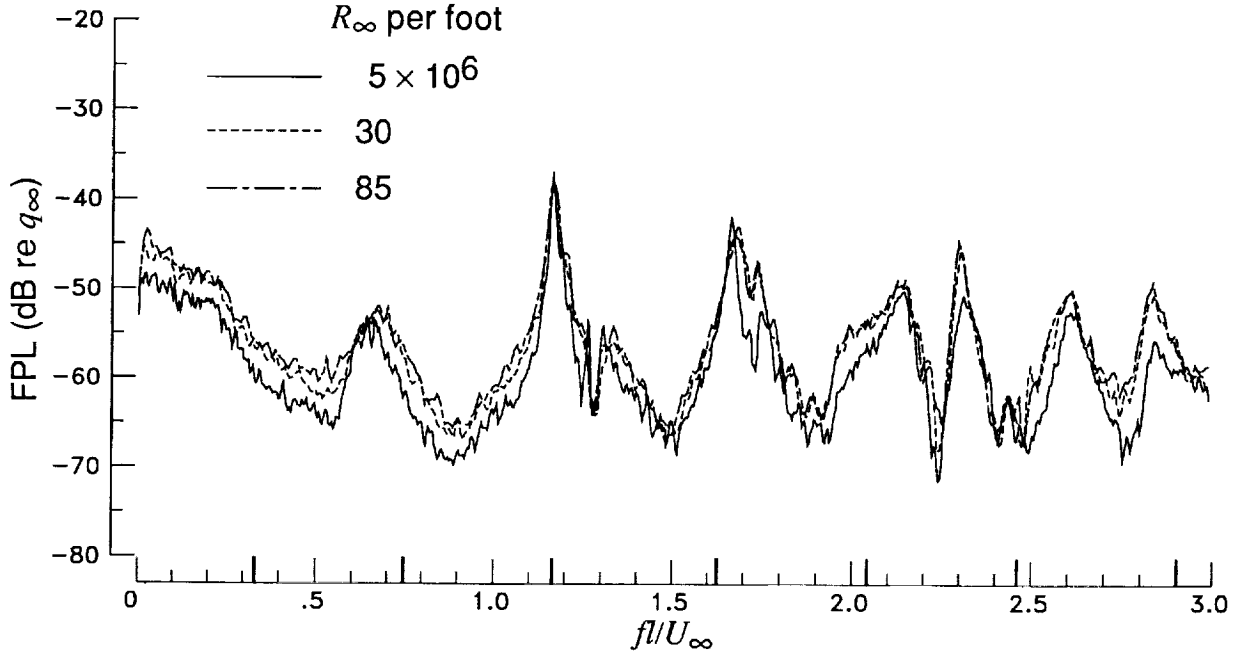

(b) $l/h = 6.70$.

Figure 6. Effect of Reynolds number on cavity fluctuating pressures for $M_\infty = 0.60$ with $\psi = 0°$. Bold ticks on the abscissa indicate modal frequencies predicted by modified Rossiter equation.

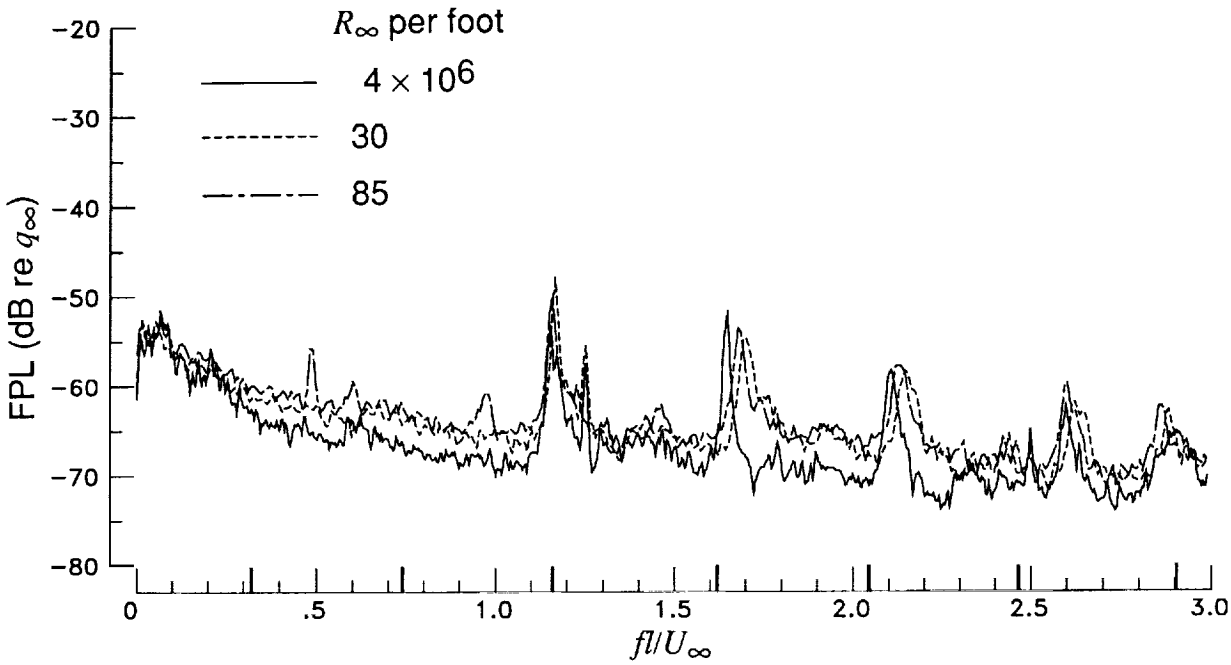

(c) $l/h = 12.67$.

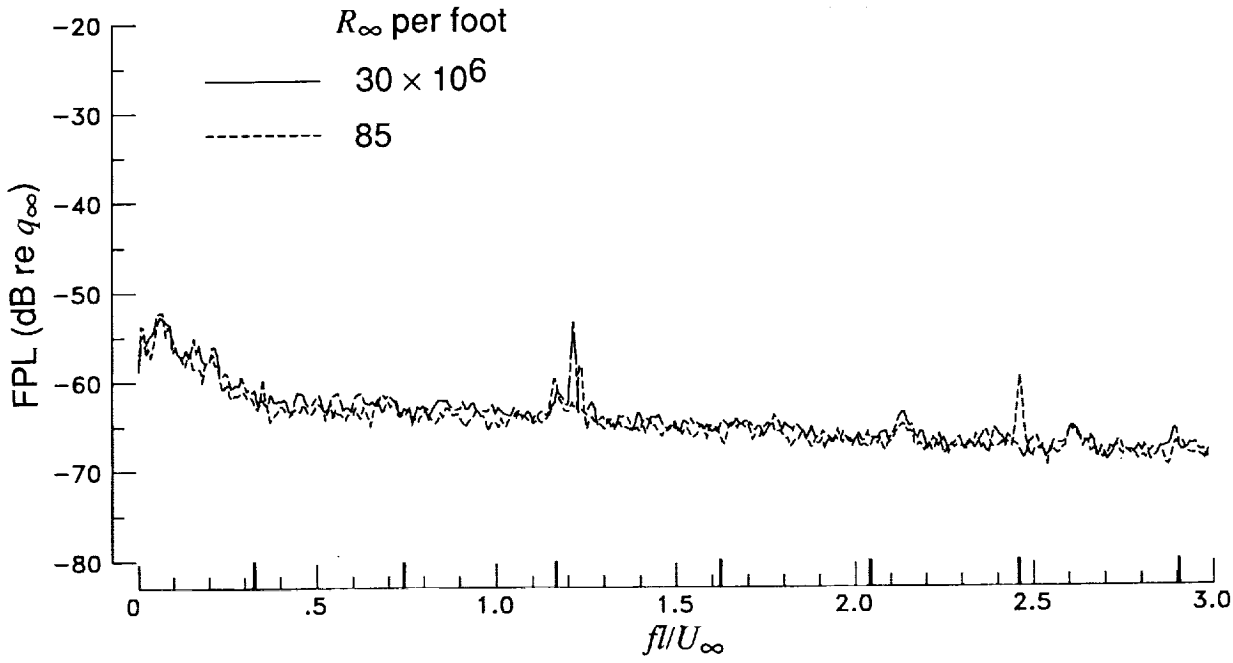

(d) $l/h = 20.00$.

Figure 6. Concluded.

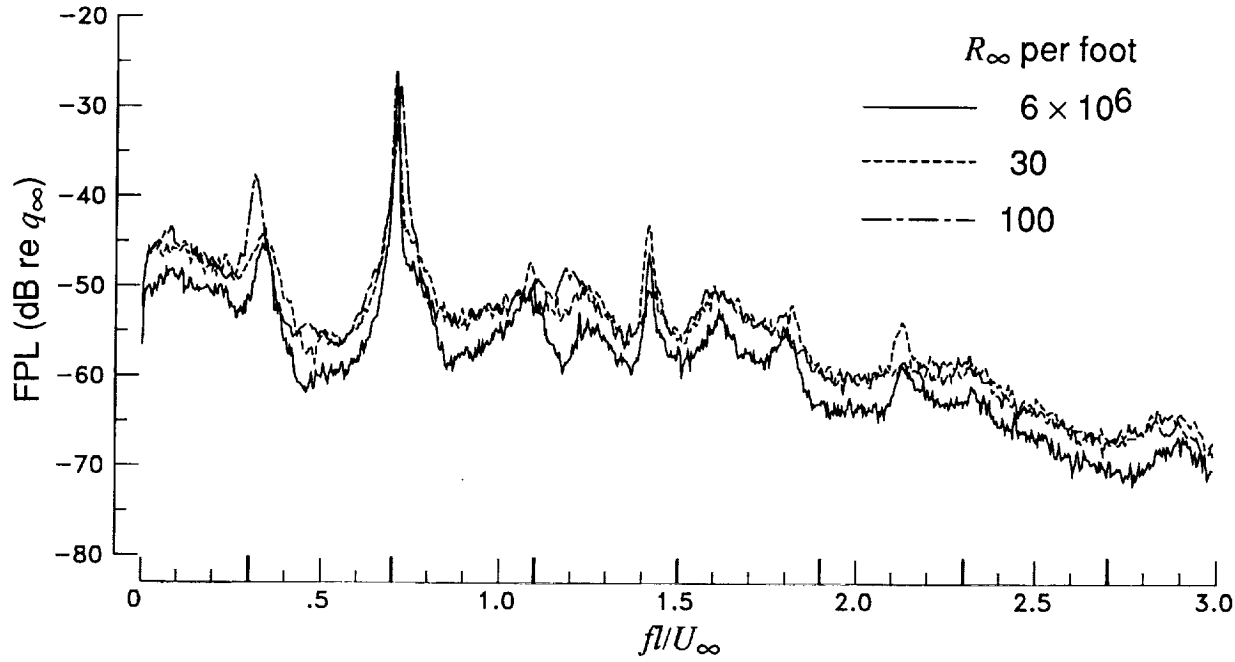

(a) $l/h = 4.40$.

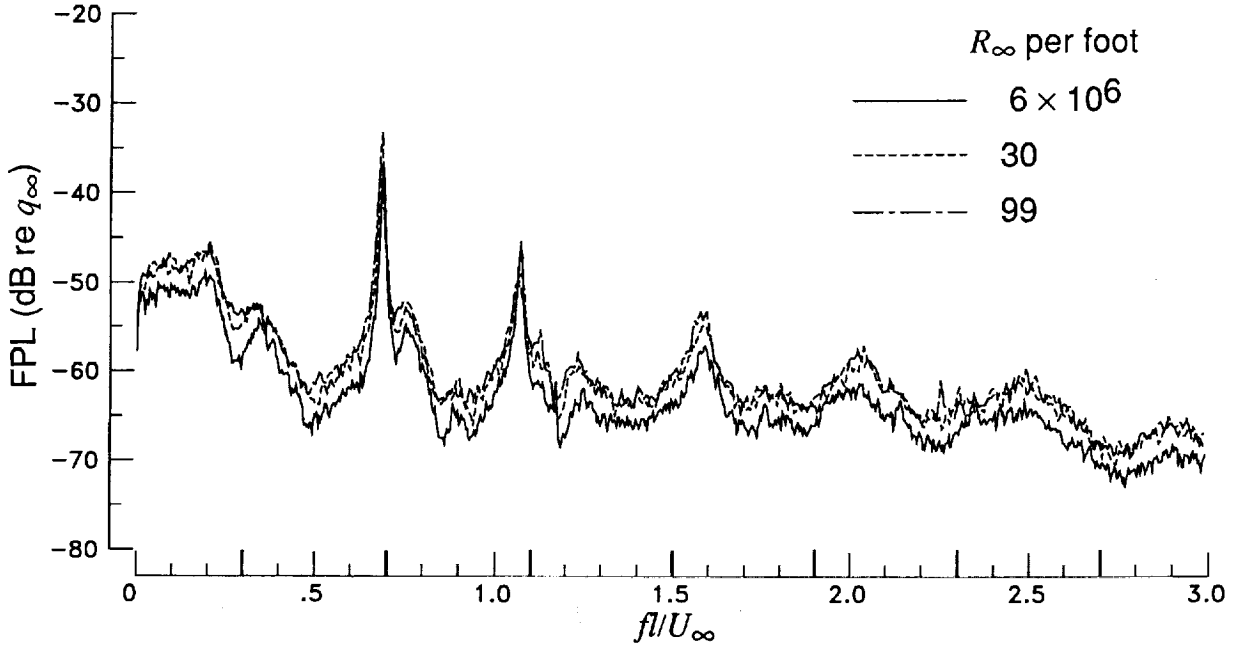

(b) $l/h = 6.70$.

Figure 7. Effect of Reynolds number on cavity fluctuating pressures for $M_\infty = 0.80$ with $\psi = 0°$. Bold ticks on the abscissa indicate modal frequencies predicted by modified Rossiter equation.

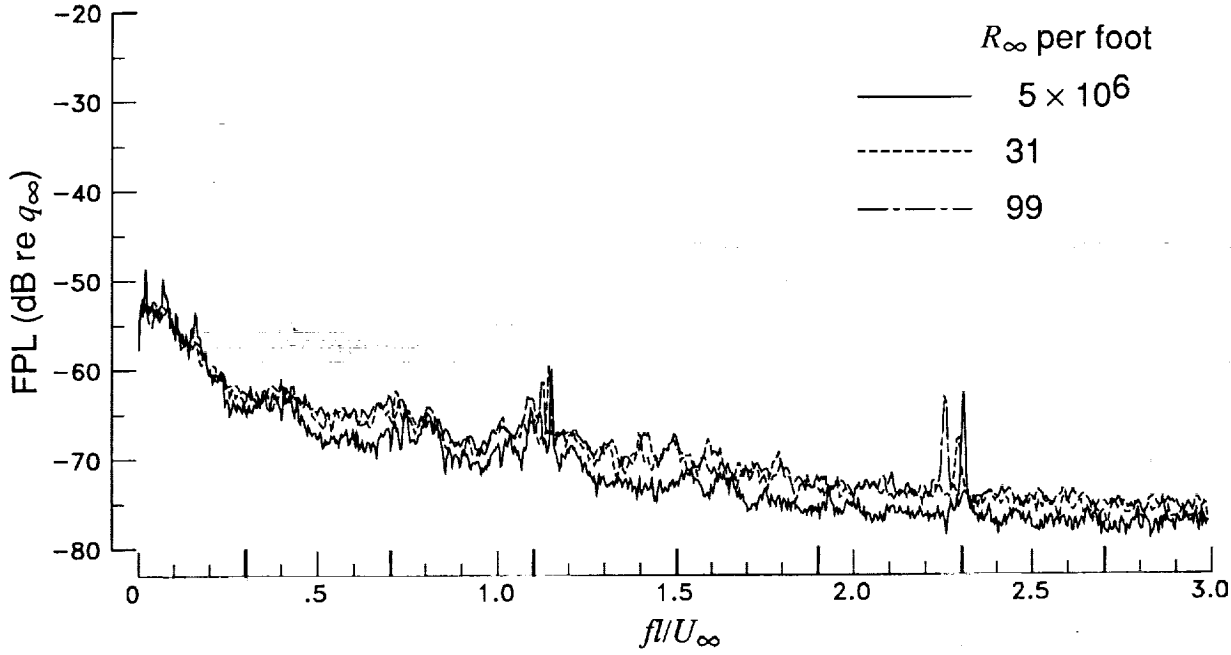

(c) $l/h = 12.67$.

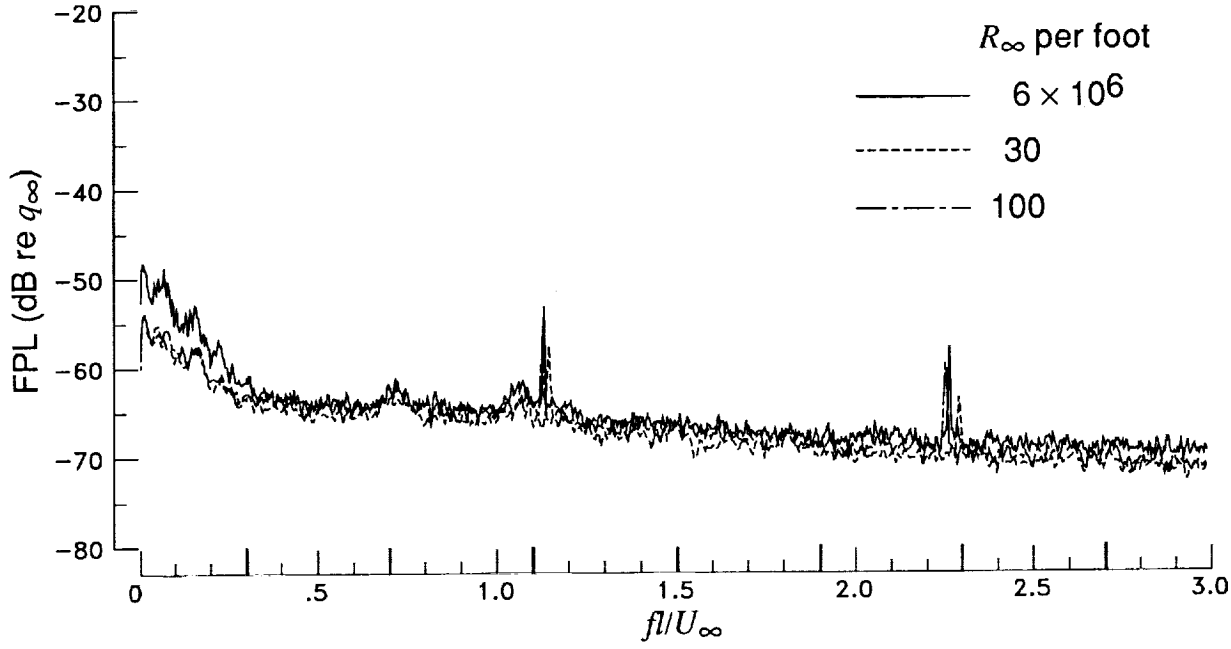

(d) $l/h = 20.00$.

Figure 7. Concluded.

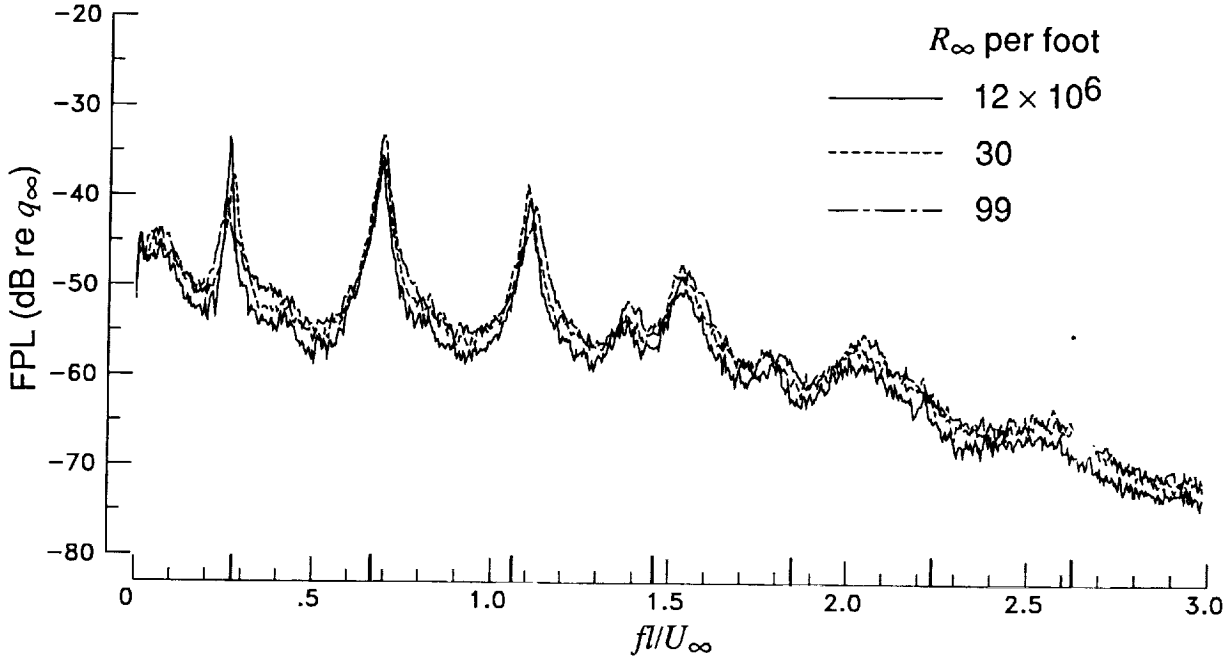

(a) $l/h = 4.40$.

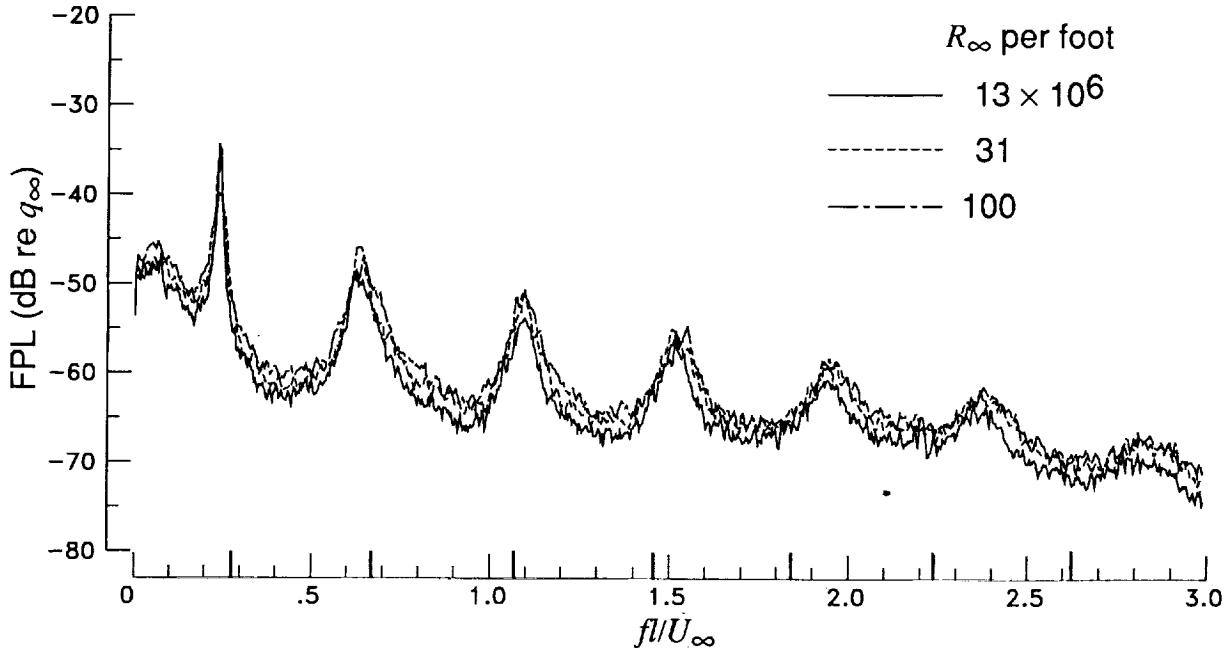

(b) $l/h = 6.70$.

Figure 8. Effect of Reynolds number on cavity fluctuating pressures for $M_\infty = 0.90$ with $\psi = 0°$. Bold ticks on the abscissa indicate modal frequencies predicted by modified Rossiter equation.

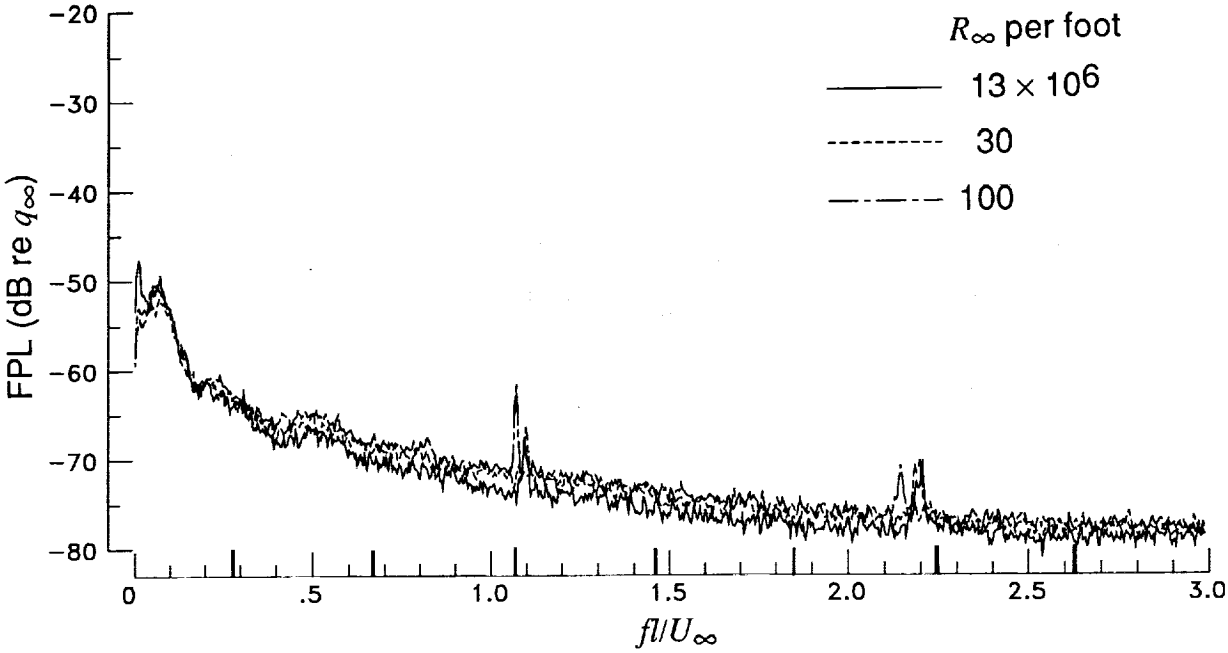

(c) $l/h = 12.67$.

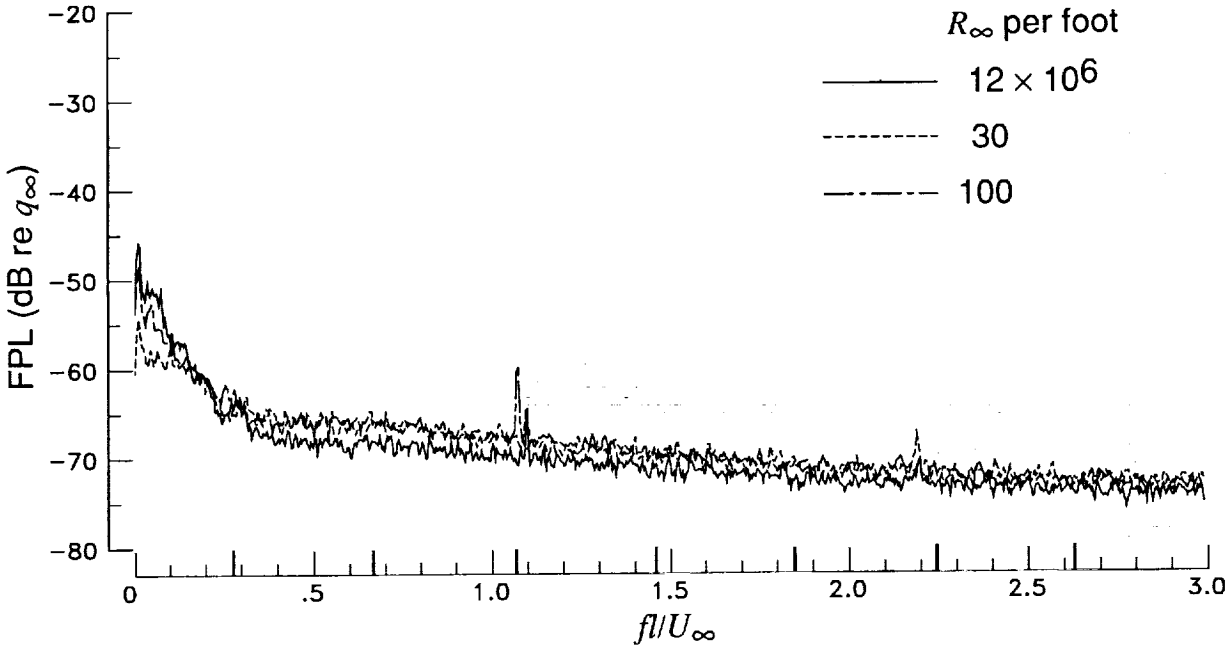

(d) $l/h = 20.00$.

Figure 8. Concluded.

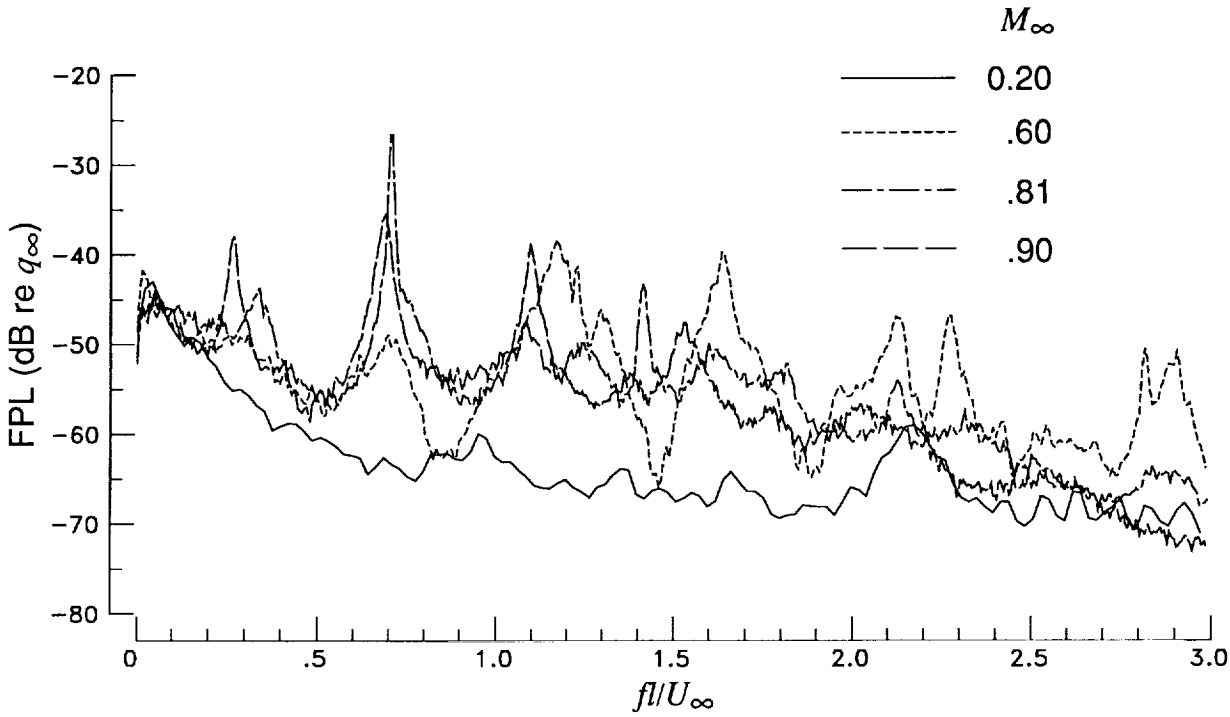

(a) $l/h = 4.40$.

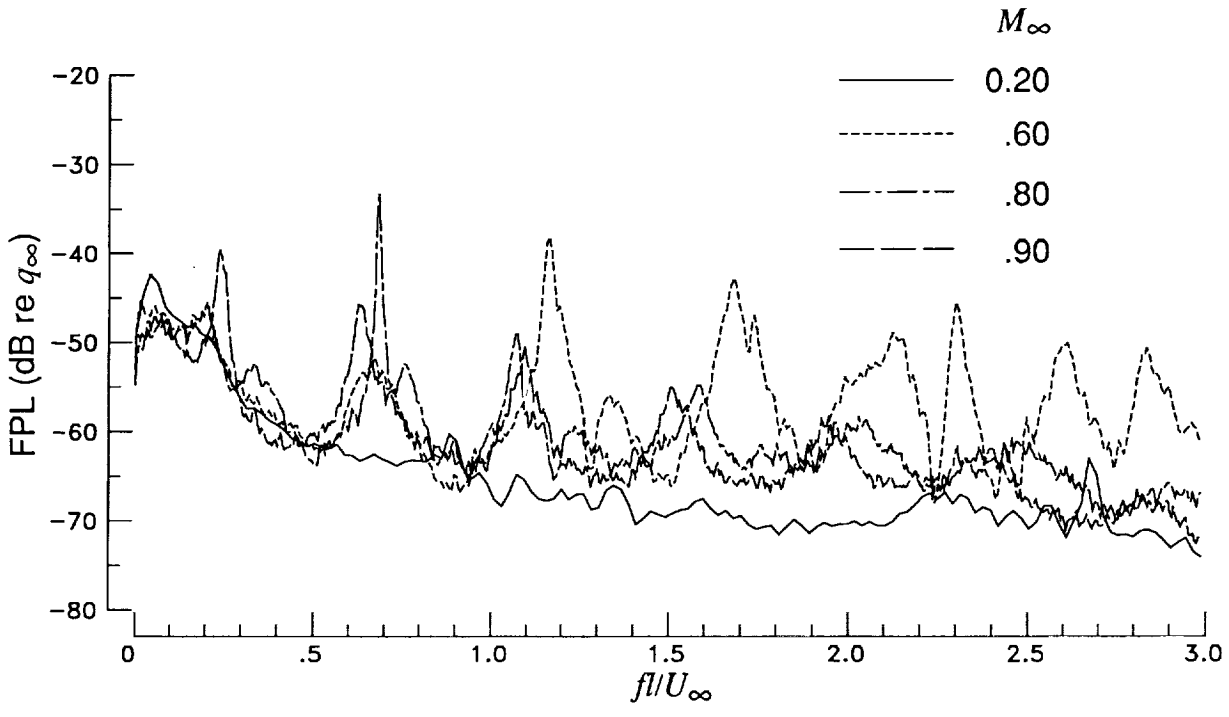

(b) $l/h = 6.70$.

Figure 9. Effect of cavity fluctuating pressures for $R_\infty = 30 \times 10^6$ per foot with $\psi = 0°$.

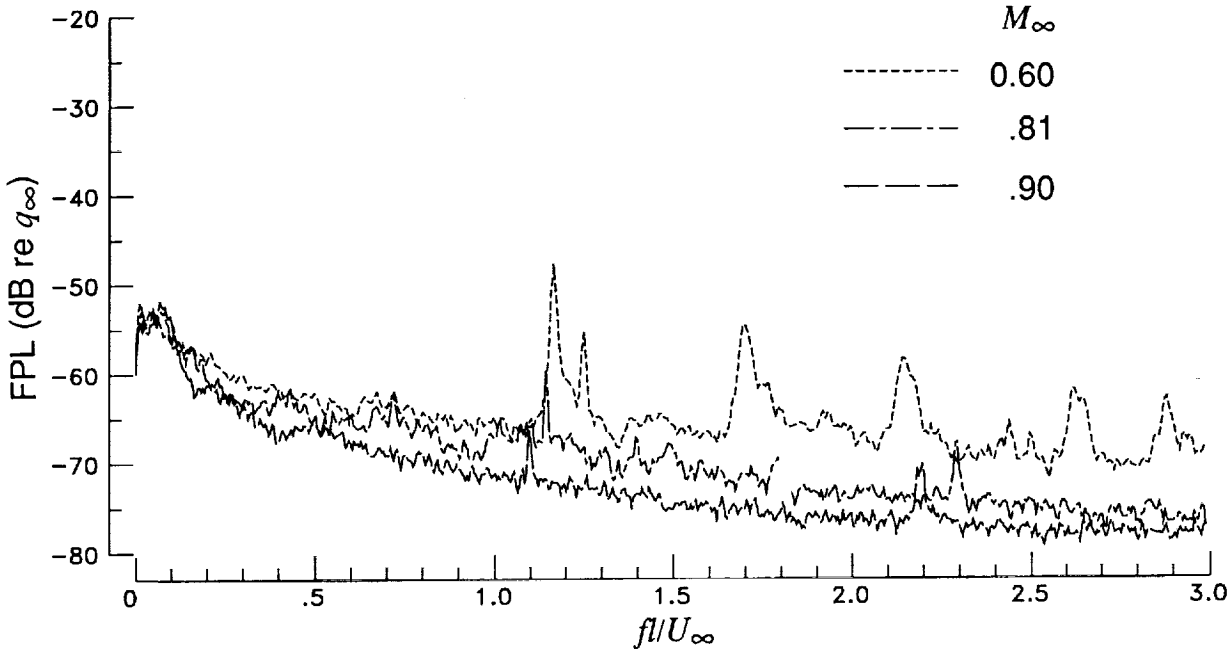

(c) $l/h = 12.67$.

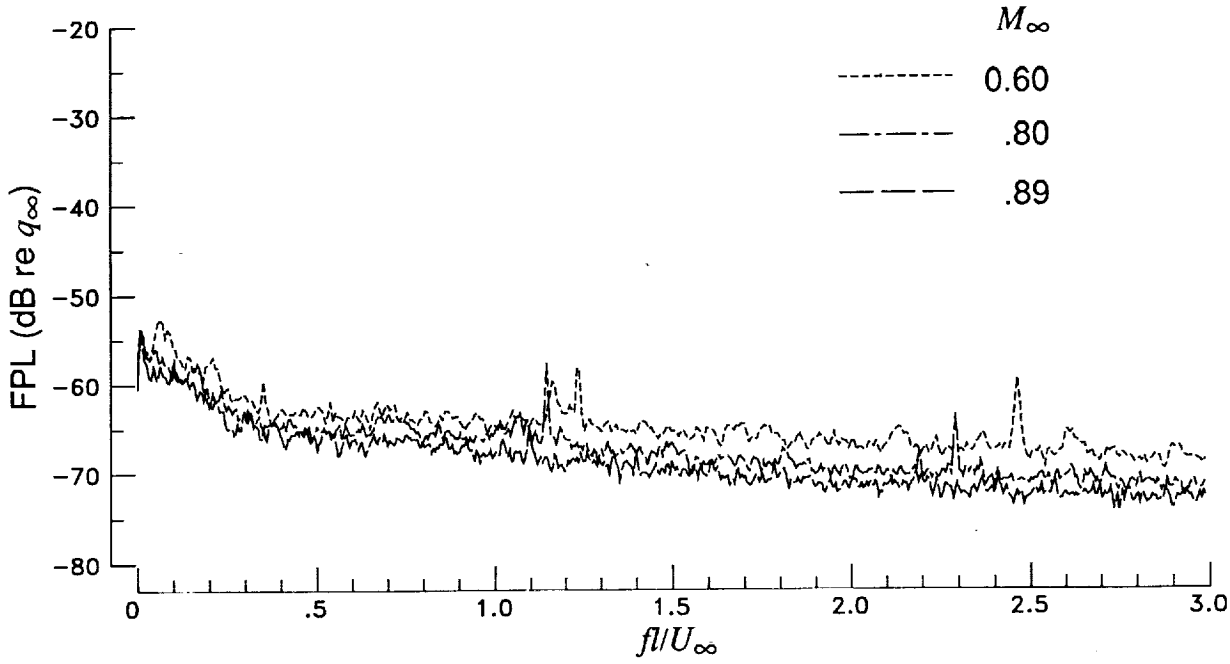

(d) $l/h = 20.00$.

Figure 9. Concluded.

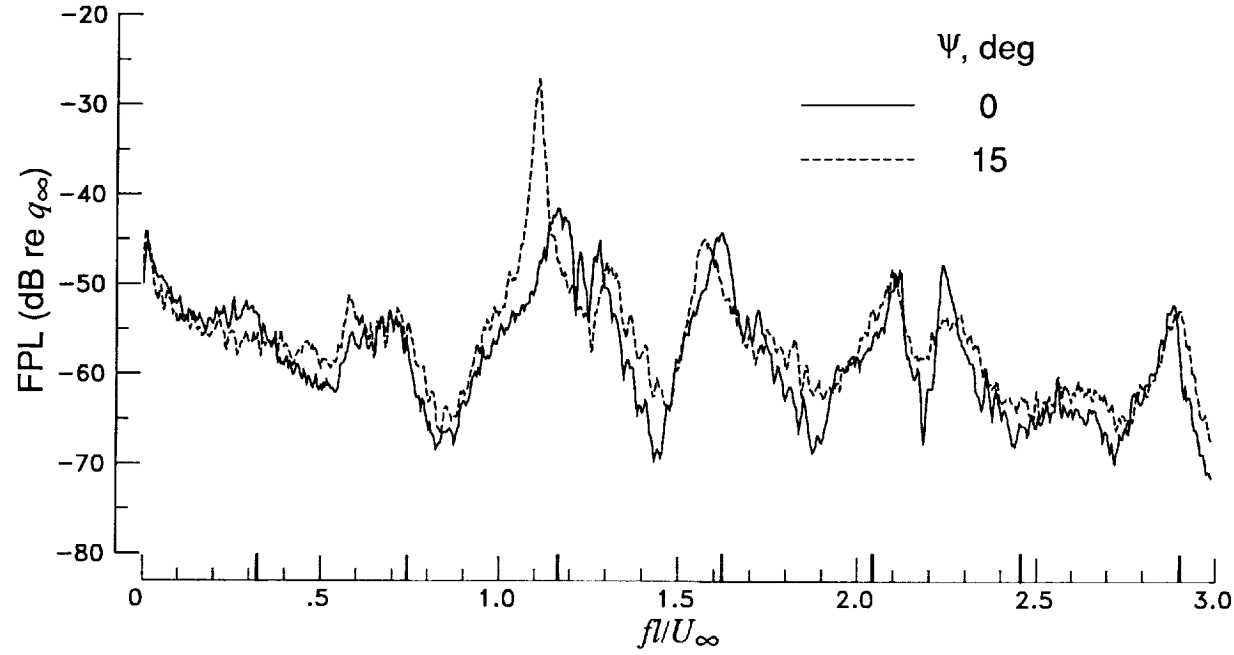

(a) $M_\infty = 0.60; R_\infty = 4 \times 10^6$ per foot.

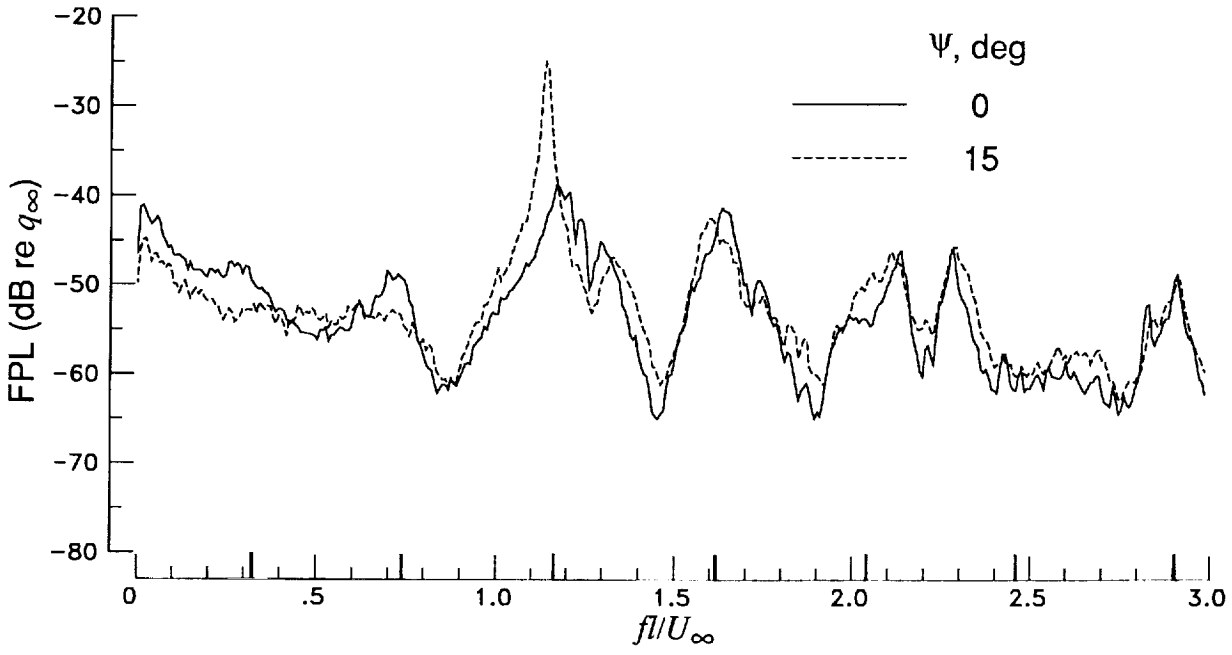

(b) $M_\infty = 0.60; R_\infty = 90 \times 10^6$ per foot.

Figure 10. Effect of angle of yaw on cavity fluctuating pressures with $l/h = 4.40$. Bold ticks on the abscissa indicate modal frequencies predicted by modified Rossiter equation.

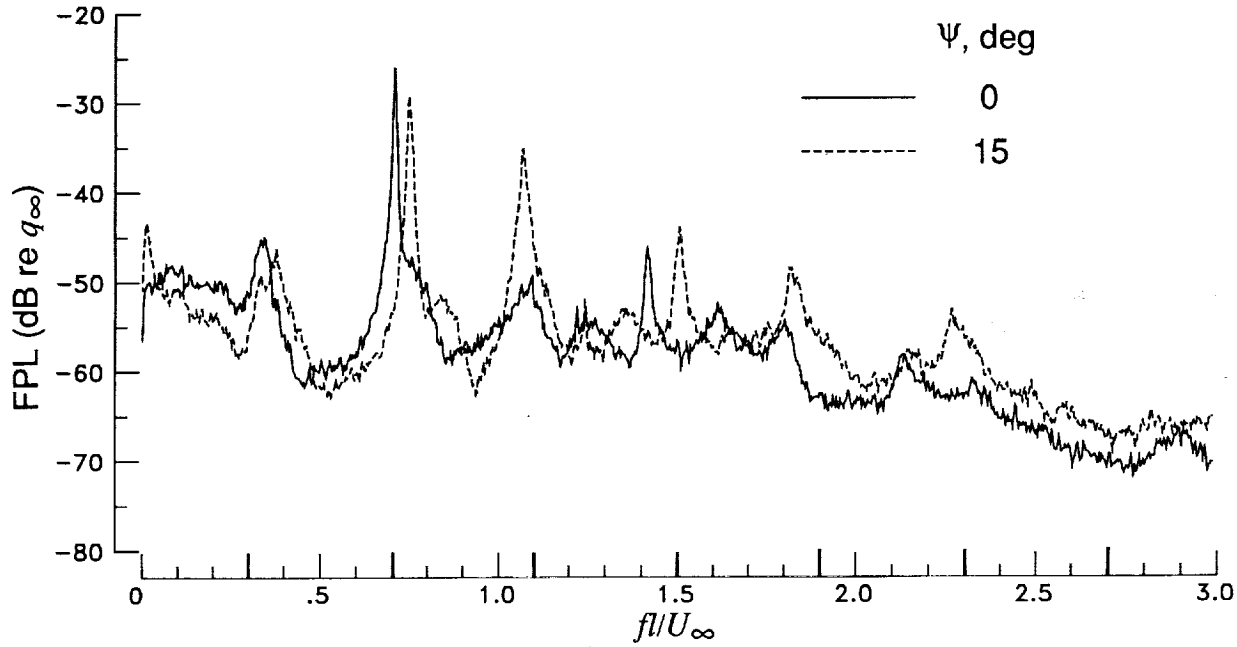

(c) $M_\infty = 0.80$; $R_\infty = 6 \times 10^6$ per foot.

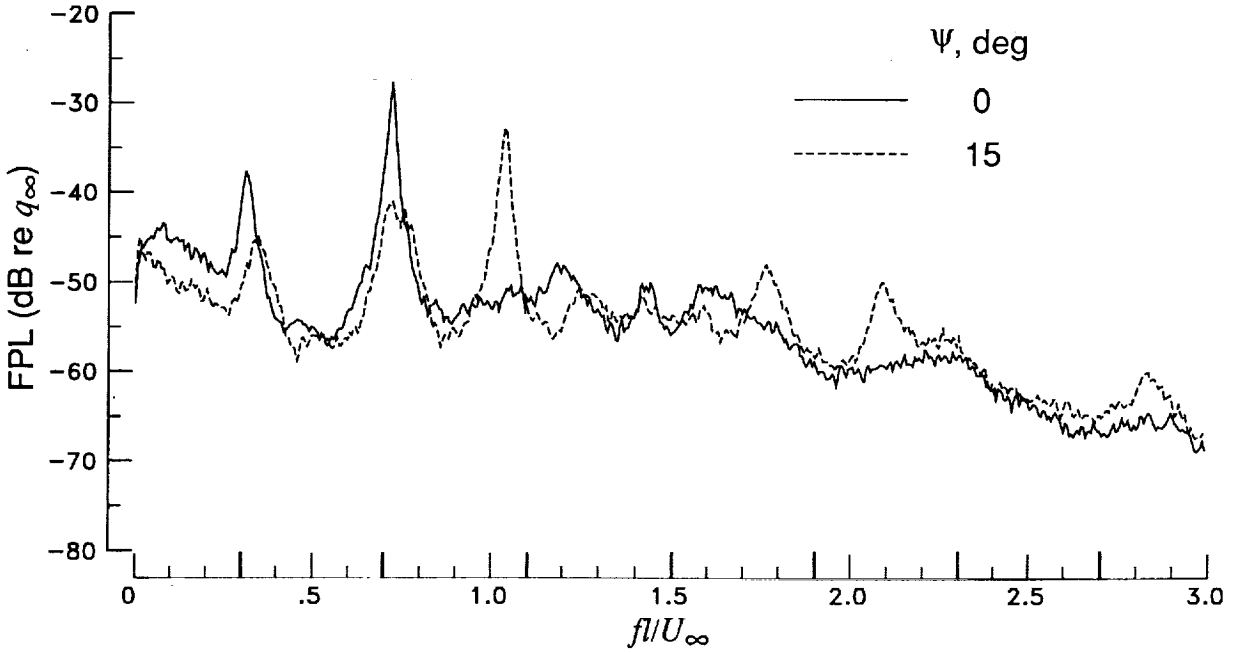

(d) $M_\infty = 0.80$; $R_\infty = 100 \times 10^6$ per foot.

Figure 10. Continued.

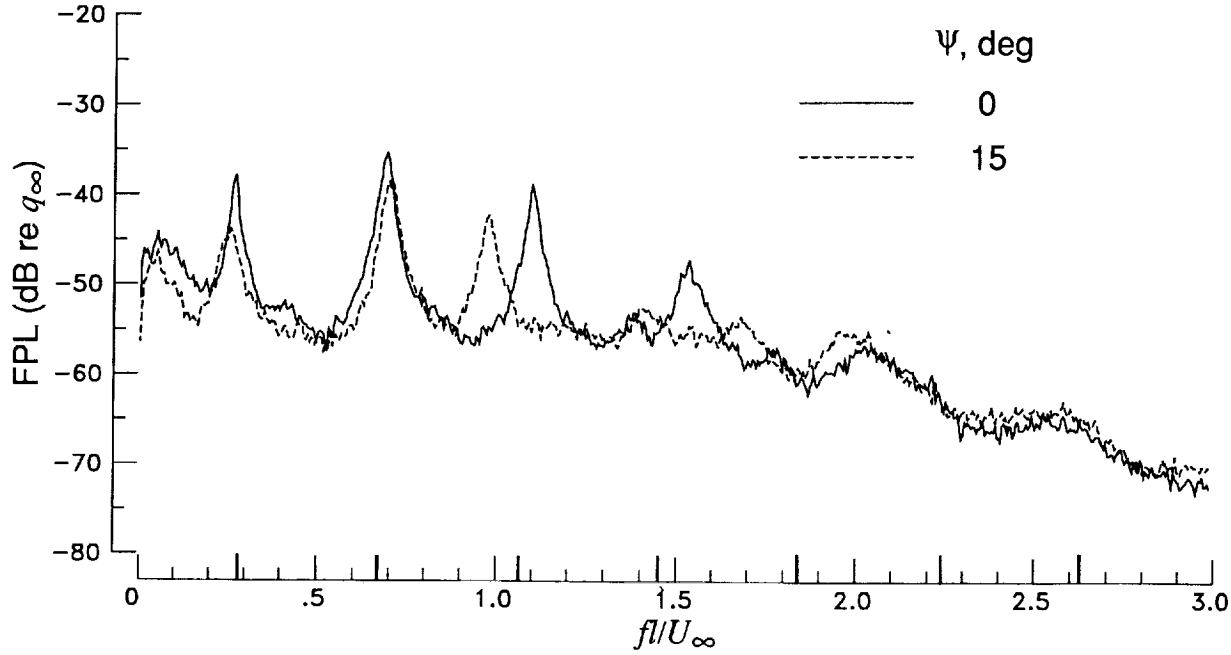

(e) $M_\infty = 0.90; R_\infty = 30 \times 10^6$ per foot.

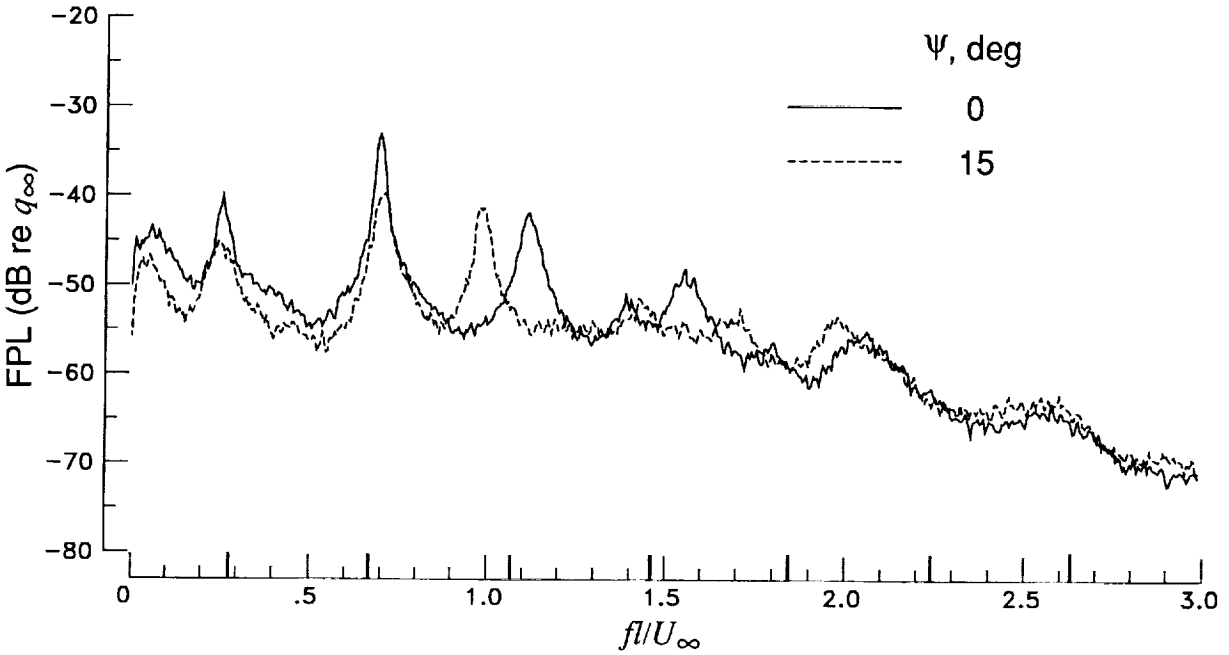

(f) $M_\infty = 0.90; R_\infty = 90 \times 10^6$ per foot.

Figure 10. Concluded.

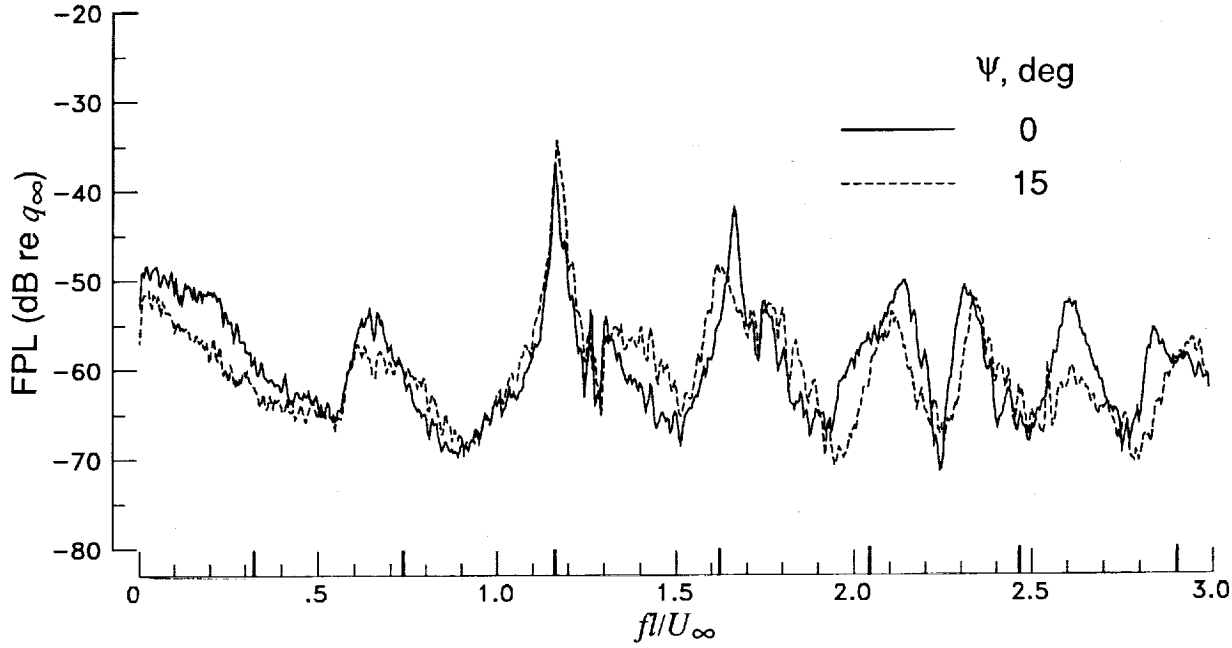

(a) $M_\infty = 0.60; R_\infty = 5 \times 10^6$ per foot.

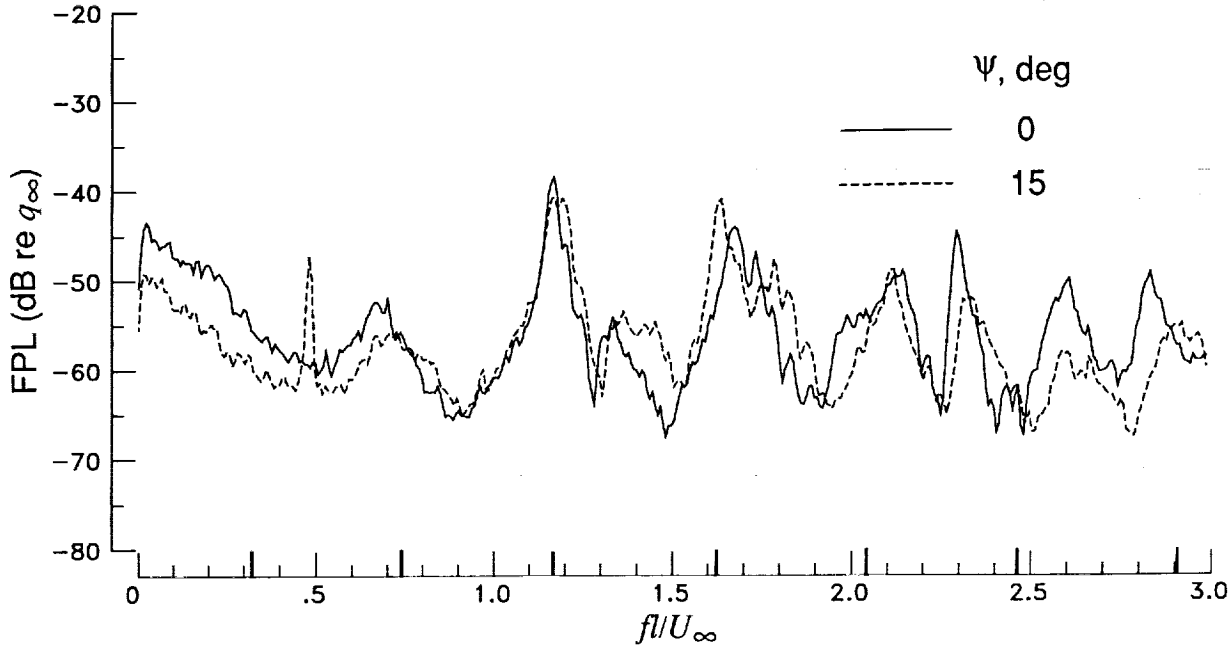

(b) $M_\infty = 0.60; R_\infty = 85 \times 10^6$ per foot.

Figure 11. Effect of angle of yaw on cavity fluctuating pressures with $l/h = 6.70$. Bold ticks on the abscissa indicate modal frequencies predicted by modified Rossiter equation.

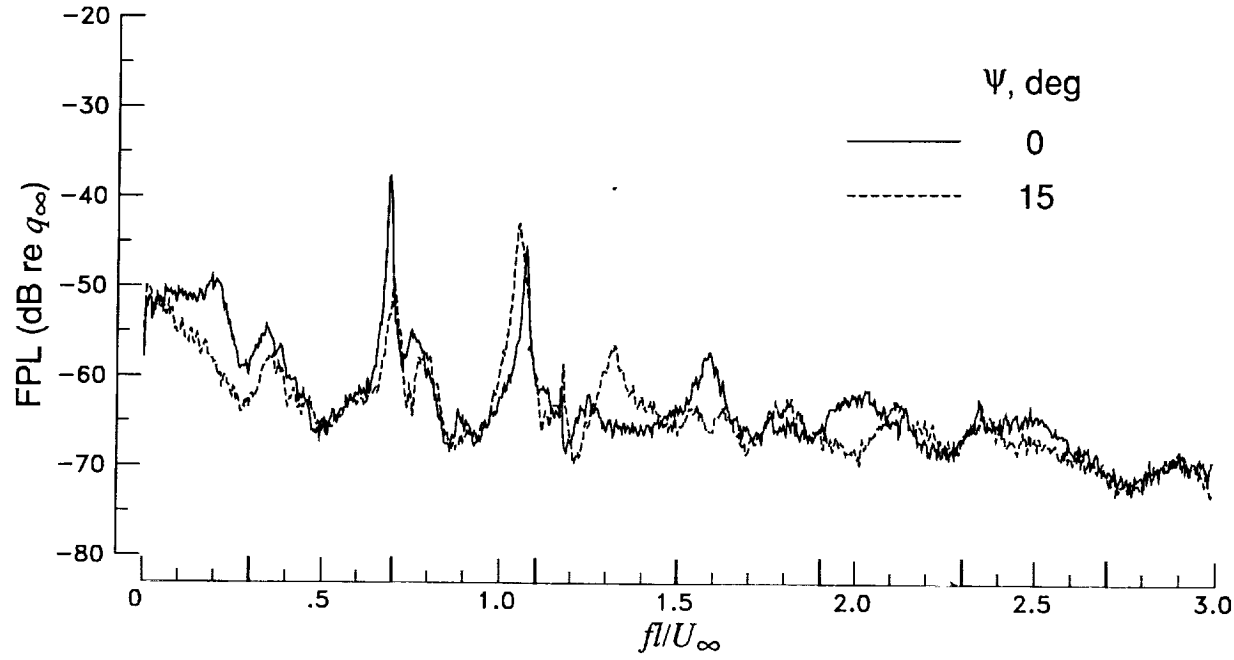

(c) $M_\infty = 0.80; R_\infty = 6 \times 10^6$ per foot.

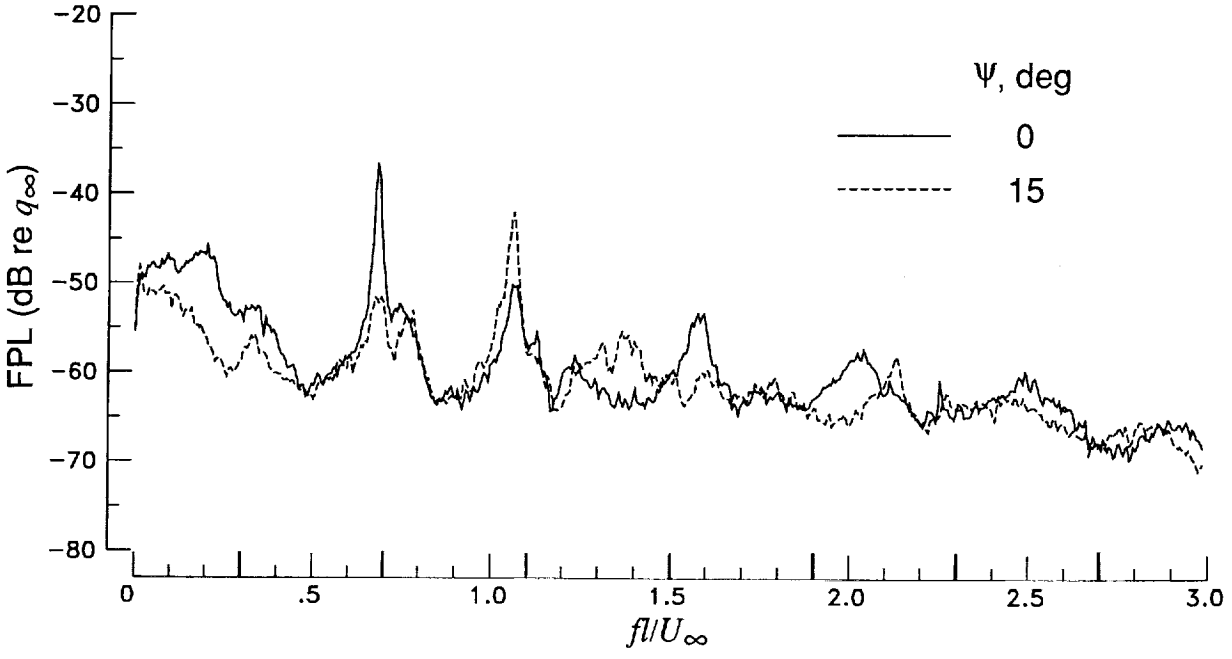

(d) $M_\infty = 0.80; R_\infty = 99 \times 10^6$ per foot.

Figure 11. Continued.

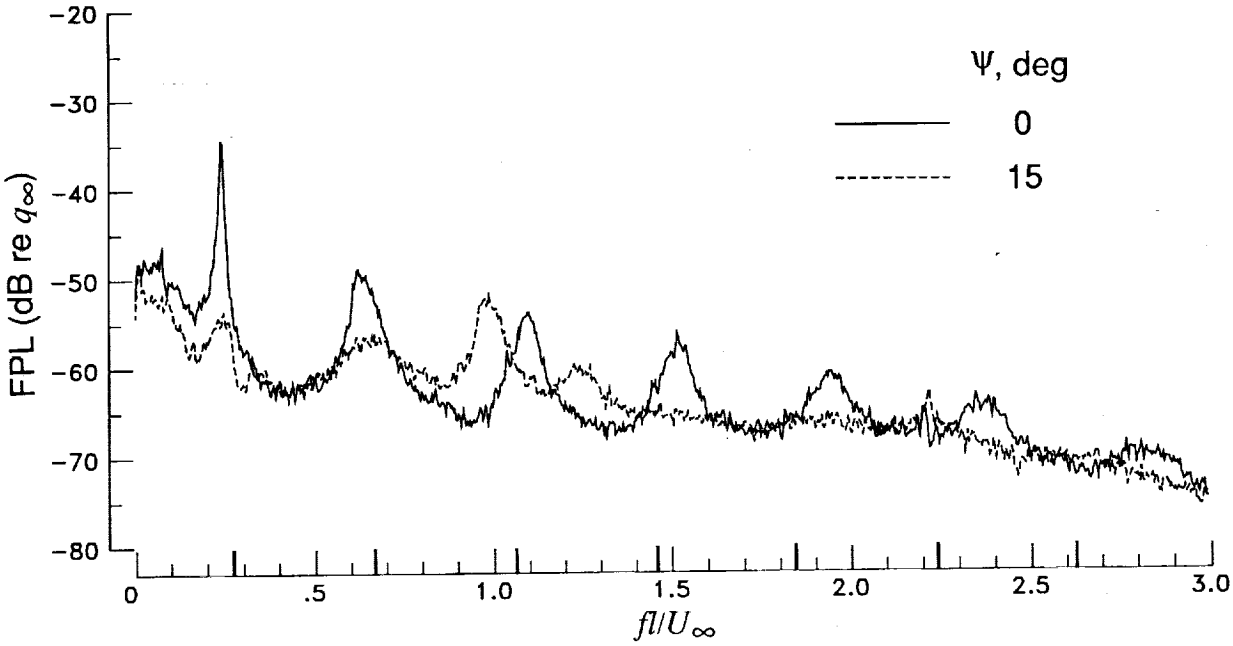

(e) $M_\infty = 0.90; R_\infty = 12 \times 10^6$ per foot.

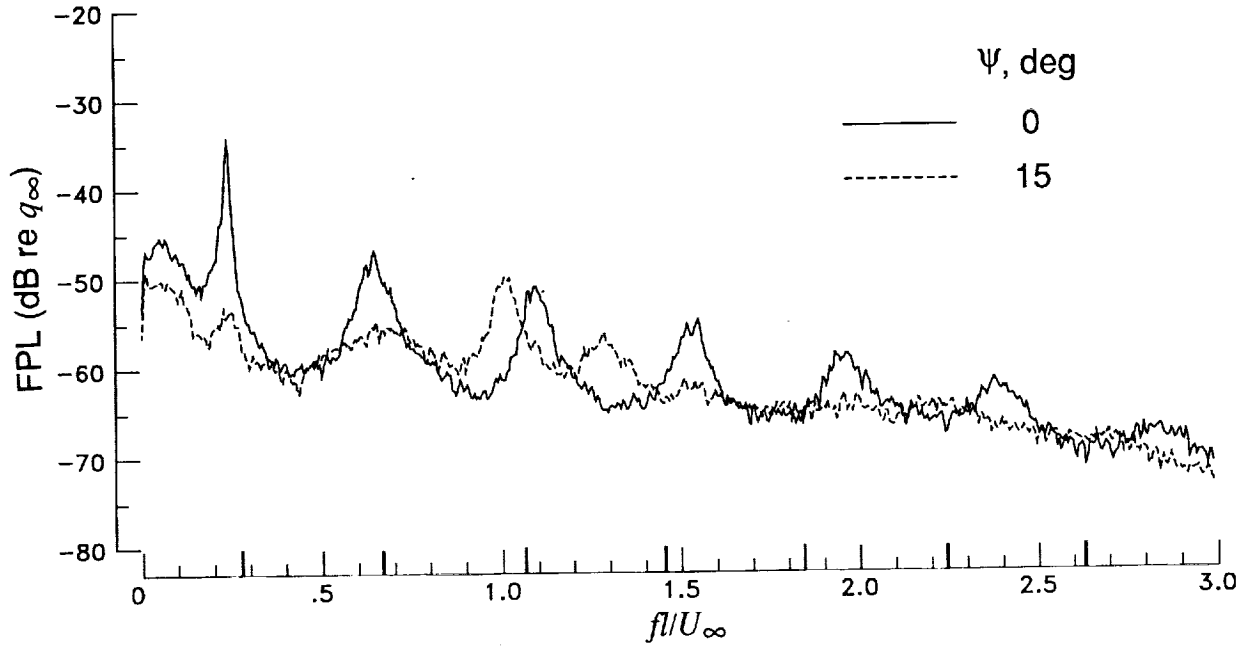

(f) $M_\infty = 0.90; R_\infty = 100 \times 10^6$ per foot.

Figure 11. Concluded.

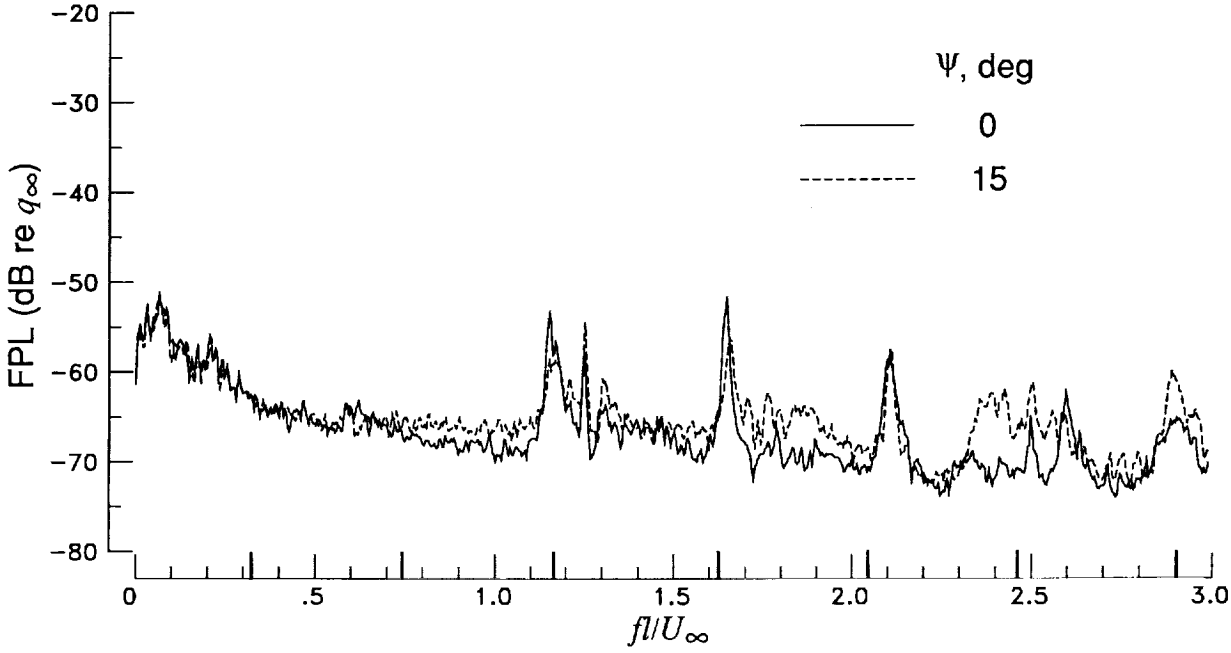

(a) $M_\infty = 0.60$; $R_\infty = 4 \times 10^6$ per foot.

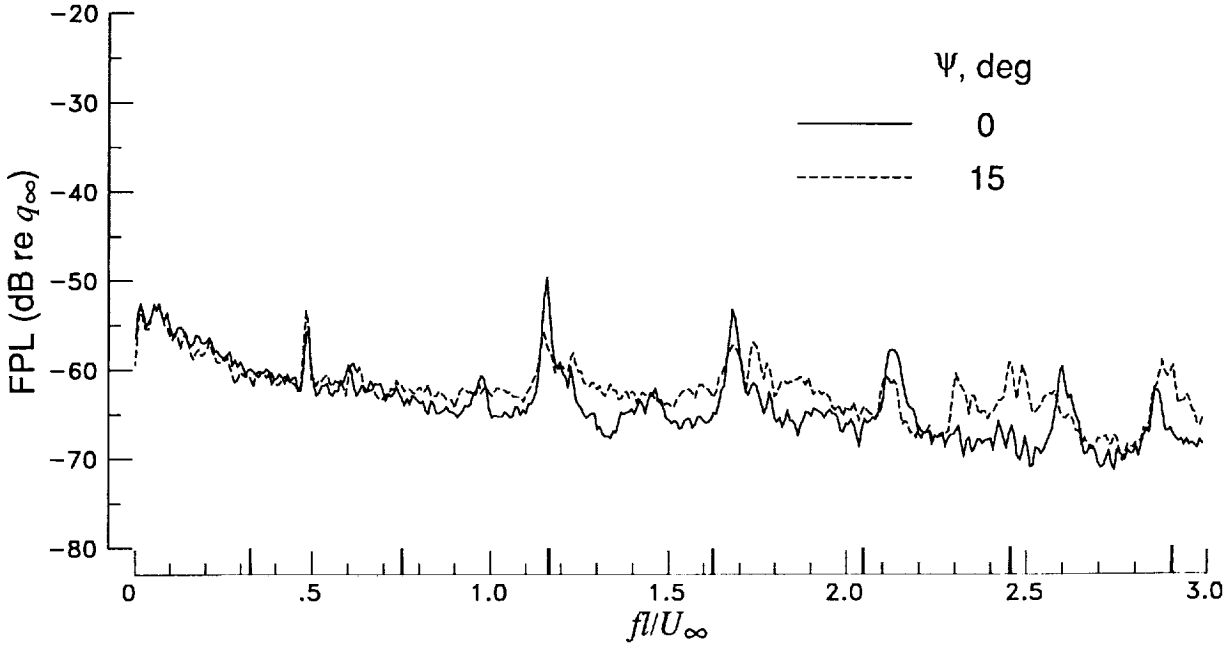

(b) $M_\infty = 0.60$; $R_\infty = 85 \times 10^6$ per foot.

Figure 12. Effect of angle of yaw on cavity fluctuating pressures with $l/h = 12.67$. Bold ticks on the abscissa indicate modal frequencies predicted by modified Rossiter equation.

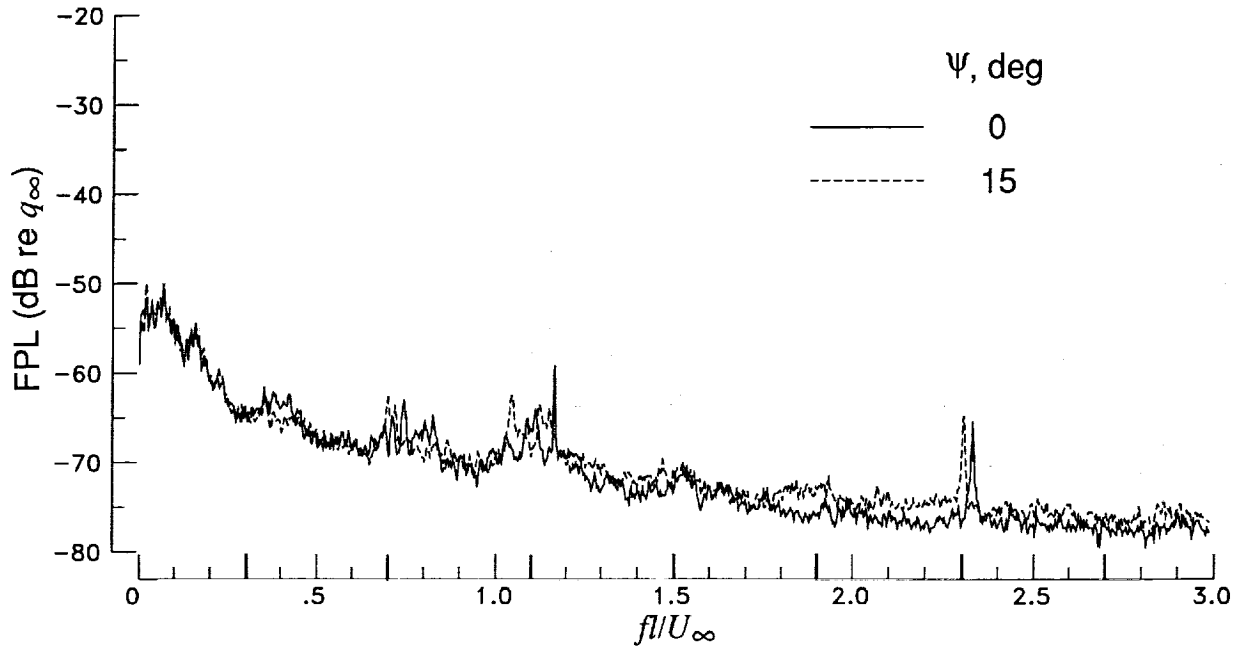

(c) $M_\infty = 0.80; R_\infty = 6 \times 10^6$ per foot.

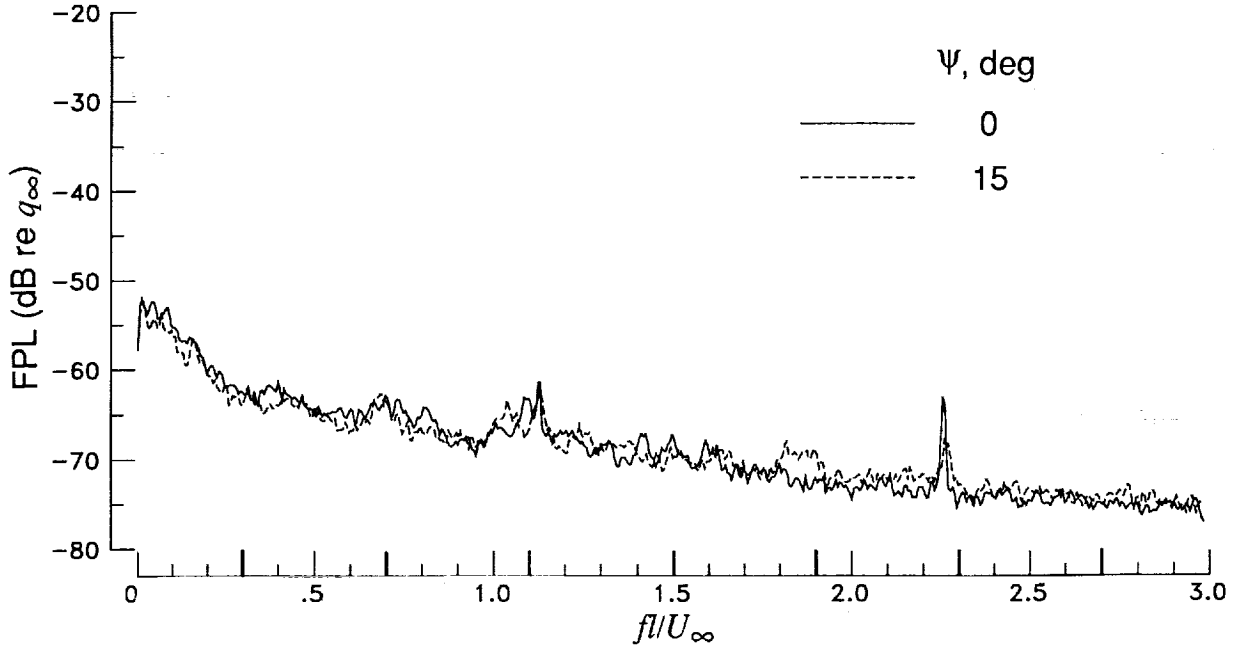

(d) $M_\infty = 0.80; R_\infty = 99 \times 10^6$ per foot.

Figure 12. Continued.

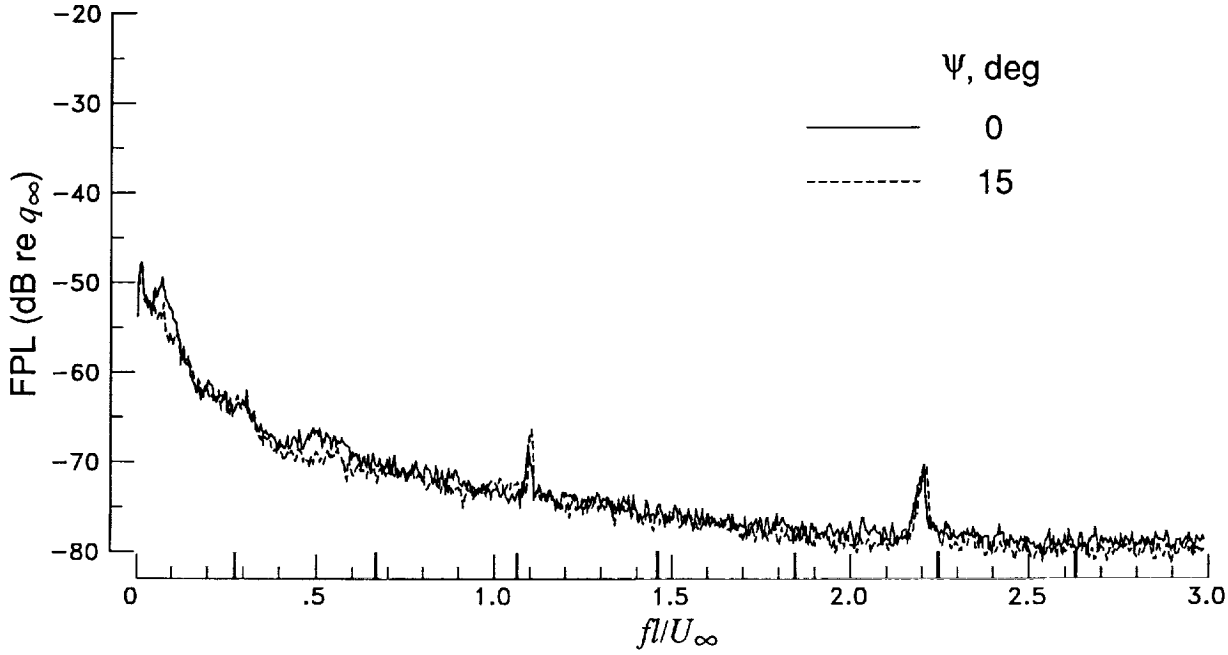

(e) $M_\infty = 0.90; R_\infty = 13 \times 10^6$ per foot.

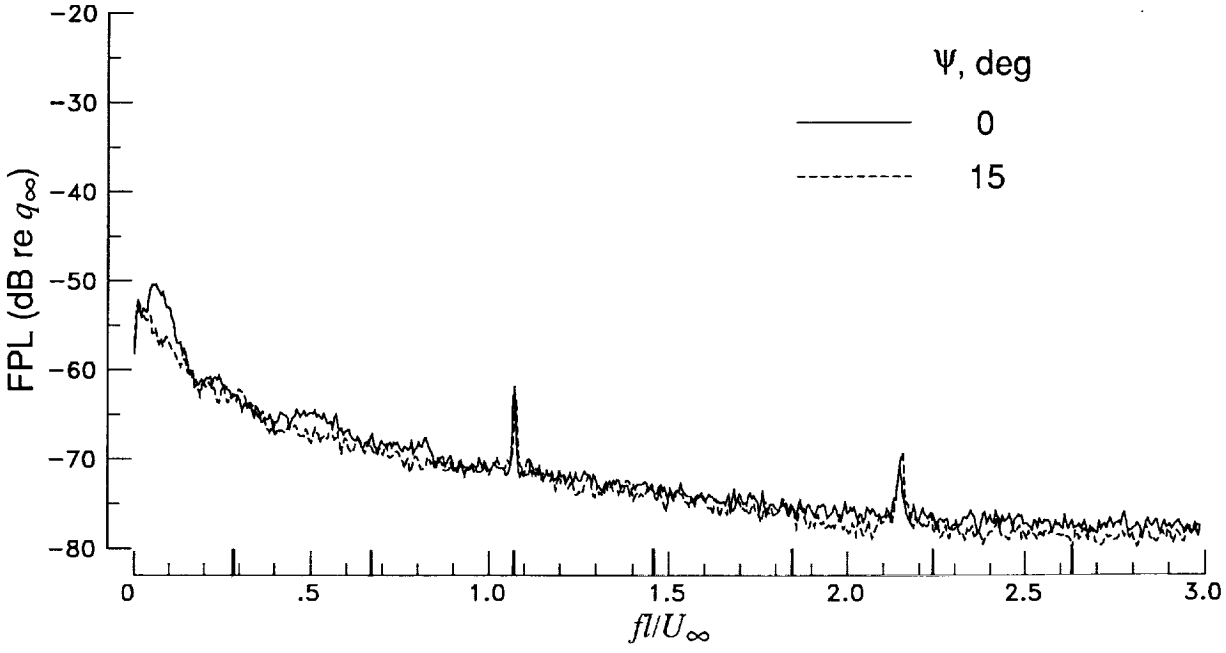

(f) $M_\infty = 0.90; R_\infty = 100 \times 10^6$ per foot.

Figure 12. Concluded.

REPORT DOCUMENTATION PAGE

Form Approved
OMB No. 0704-0188

1. AGENCY USE ONLY *(Leave blank)*	2. REPORT DATE	3. REPORT TYPE AND DATES COVERED
	June 1992	Technical Memorandum

4. TITLE AND SUBTITLE
Measurements of Fluctuating Pressure in a Rectangular Cavity in Transonic Flow at High Reynolds Numbers

5. FUNDING NUMBERS
WU 505-68-70-08

6. AUTHOR(S)
M. B. Tracy, E. B. Plentovich, and Julio Chu

7. PERFORMING ORGANIZATION NAME(S) AND ADDRESS(ES)
NASA Langley Research Center
Hampton, VA 23665-5225

8. PERFORMING ORGANIZATION REPORT NUMBER
L-16859

9. SPONSORING/MONITORING AGENCY NAME(S) AND ADDRESS(ES)
National Aeronautics and Space Administration
Washington, DC 20546-0001

10. SPONSORING/MONITORING AGENCY REPORT NUMBER
NASA TM-4363

11. SUPPLEMENTARY NOTES

12a. DISTRIBUTION/AVAILABILITY STATEMENT
Unclassified Unlimited

Subject Category 02

12b. DISTRIBUTION CODE

13. ABSTRACT *(Maximum 200 words)*

An experiment was performed in the Langley 0.3-Meter Transonic Cryogenic Tunnel to study the internal acoustic field generated by rectangular cavities in transonic and subsonic flows and to determine the effect of Reynolds number and angle of yaw on the field. The cavity in this study was 11.25 in. long and 2.50 in. wide. The cavity depth was varied to obtain length-to-height (l/h) ratios of 4.40, 6.70, 12.67, and 20.00. Data were obtained for a free-stream Mach number (M_∞) range from 0.20 to 0.90, a Reynolds number range from 2×10^6 to 100×10^6 per foot with a nearly constant boundary-layer thickness, and for two angles of yaw of 0° and 15°. Results show that Reynolds number has little effect on the acoustic field in rectangular cavities at an angle of yaw of 0°. Cavities with $l/h = 4.40$ and 6.70 generated tones at transonic speeds, whereas those with $l/h = 20.00$ did not. This trend agrees with data obtained previously at supersonic speeds. As M_∞ decreased, the amplitude and bandwidth of the tones changed. No tones appeared for $M_\infty = 0.20$. For a cavity with $l/h = 12.67$, tones appeared at $M_\infty = 0.60$, indicating a possible change in flow-field type. Changes in acoustic spectra with angle of yaw varied with Reynolds number, M_∞, l/h ratios, and acoustic mode number.

14. SUBJECT TERMS
Cavity acoustics; High Reynolds numbers; Transonic speeds; Unsteady flow

15. NUMBER OF PAGES
30

16. PRICE CODE
A03

17. SECURITY CLASSIFICATION OF REPORT	18. SECURITY CLASSIFICATION OF THIS PAGE	19. SECURITY CLASSIFICATION OF ABSTRACT	20. LIMITATION OF ABSTRACT
Unclassified	Unclassified		